

1. Report No. NASA CR-2399		2. Government Accession No.		3. Recipient's Catalog No.	
4. Title and Subtitle COMPUTER PROGRAM FOR THIN-WIRE STRUCTURES IN A HOMOGENEOUS CONDUCTING MEDIUM		5. Report Date June 1974		6. Performing Organization Code	
7. Author(s) J. H. Richmond		8. Performing Organization Report No. TR 2902-12		10. Work Unit No. 502-33-13-02	
9. Performing Organization Name and Address The Ohio State University ElectroScience Laboratory Columbus, Ohio 43212		11. Contract or Grant No. NRI 36-008-138		13. Type of Report and Period Covered Contractor Report	
12. Sponsoring Agency Name and Address National Aeronautics and Space Administration Washington, D.C. 20546		14. Sponsoring Agency Code			
15. Supplementary Notes Topical report.					
16. Abstract A computer program is presented for thin-wire antennas and scatterers in a homogeneous conducting medium. The analysis is performed in the real or complex frequency domain. The program handles insulated and bare wires with finite conductivity and lumped loads. The output data includes the current distribution, impedance, radiation efficiency, gain, absorption cross section, scattering cross section, echo area and the polarization scattering matrix. The program uses sinusoidal bases and Galerkin's method.					
17. Key Words (Suggested by Author(s)) Antennas, Spacecraft and Aircraft Antennas Applied Electromagnetic Theory		18. Distribution Statement Unclassified - Unlimited			
18. Security Classif. (of this report) Unclassified		20. Security Classif. (of this page) Unclassified		21. No. of Pages 52	22. Price* \$3.75



\* For sale by the National Technical Information Service, Springfield, Virginia 22161

## CONTENTS

I.	INTRODUCTION	1
II.	THE THIN-WIRE COMPUTER PROGRAM	2
III.	SUMMARY	17
REFERENCES		
APPENDIX 1	Subroutine SORT	19
APPENDIX 2	Subroutine SGANT	19
APPENDIX 3	Subroutine CBES	19
APPENDIX 4	Subroutine DSHLL	25
APPENDIX 5	Subroutine GGS	25
APPENDIX 6	Subroutine GGM	30
APPENDIX 7	Subroutine EXPJ	34
APPENDIX 8	Subroutine GANT1	37
APPENDIX 9	Subroutine SQROT	37
APPENDIX 10	Subroutine RITE	40
APPENDIX 11	Subroutine GDISS	42
APPENDIX 12	Subroutine GNFLD	42
APPENDIX 13	Subroutine GNF	42
APPENDIX 14	Subroutine GFLD	42
APPENDIX 15	Subroutine GFF	49

## I. INTRODUCTION

Reference 1 presents the electromagnetic theory for a thin-wire structure in a homogeneous conducting medium, and this report presents the corresponding computer program. The program performs a frequency-domain analysis of thin-wire antennas and scatterers. The wire configuration is a generalized polygon assembled from straight wire segments. The program has been tested extensively with simple structures (linear dipoles, V dipoles, coupled dipoles, square loops, octagonal loops, multiturn loops and coupled loops) and complicated configurations including wire-grid models of plates, spheres, cones, aircraft and ships. Although the air-earth or air-water interface is not considered, the program is applicable in many problems involving buried or submerged antennas or targets. It is useful in locating the poles of the admittance or scattering function for wire structures in the complex frequency domain.

A piecewise-sinusoidal expansion is used for the current distribution. The matrix equation  $ZI = V$  is generated by enforcing reaction tests with a set of sinusoidal dipoles located in the interior region of the wire. Since the test dipoles have the same current distribution as the expansion modes, this may be regarded as an application of Galerkin's method. Rumsey's reaction concept was most helpful in this development, and therefore the formulation is known as the "sinusoidal reaction technique."

The current is assumed to vanish at the endpoints (if any) of the wire, and Kirchhoff's current law is enforced everywhere on the structure. The input data specify the frequency, wire radius, wire conductivity, the parameters of the exterior medium, coordinates of points to describe the shape and size of the wire configuration, and a list of the wire segments. If some or all of the wire segments are insulated, the radius and permittivity of the insulating sleeve are indicated.

Coordinates are required for wire endpoints, corners, junctions and terminals. For accuracy, the longest wire segment should not greatly exceed one-quarter wavelength. Longer segments should be subdivided by defining additional current-sampling points. The program automatically defines a set of  $N$  sinusoidal dipole modes on the wire structure and computes the mutual impedance matrix for these modes. The elements in the matrix are generated by numerical integration when appropriate, or from closed-form expressions in terms of exponential integrals. The computer program uses certain approximations which yield a symmetric matrix even when the wire structure has finite conductivity, lumped loads and insulating sleeves.

In antenna problems, the output data includes the current distribution, impedance, radiation efficiency, gain, patterns and near-zone field. In bistatic scattering problems, the output includes the echo

area and the complex elements of the polarization scattering matrix. In backscatter situations, the output includes also the absorption, scattering and extinction cross sections.

If the wire has finite conductivity or dielectric sleeves, it is assumed that the frequency is real. This restriction can readily be removed if the user will specify the surface impedance of the wire and the complex permittivities of the dielectric sleeves and the ambient medium appropriate for complex frequencies.

The user may make a tradeoff between accuracy and computation costs by specifying the input variable INT. A large value increases the accuracy and the cost. For most problems, the recommended value is INT = 4.

The program was run on an IBM 370/165 computer to determine the broadside backscatter for a wire-grid square plate with edge length L. With a five-by-five grid, there are 60 segments, 36 points and 84 simultaneous equations. With INT = 4, calculations were made for  $L/\lambda = 0.3, 0.4, 0.5, 0.6$  and  $0.7$ . The execution time was 100 seconds. This averages to 20 seconds for each value of  $L/\lambda$ . The wire structure was perfectly conducting, uninsulated and located in free space. No advantage was taken of the target symmetries.

The next section presents the thin-wire computer program, instructions for the user, typical input and output data and tables of the mutual impedance and explain their functions.

## II. THE THIN-WIRE COMPUTER PROGRAM

Fig. 1 is a Fortran listing of the thin-wire computer program. Near the beginning of this program, the DIMENSION statements reserve storage for a wire structure with up to 50 segments, 55 points and 60 dipole modes. Quantities with the same or related dimensions are grouped together on the same line or consecutive lines.

NM denotes the actual number of monopoles (segments), INM is the corresponding dimension, and the dimension for CG, VG and ZLD is twice INM. The second subscript for MD always has a dimension of 4.

N denotes the number of simultaneous linear equations and ICJ is the corresponding dimension. The dimension for C is  $(ICJ*ICJ) + ICJ/2$ .

The DO LOOP ending at statement 15 sets  $ISC(J) = 0$  for all the segments. This indicates that the wires are bare or uninsulated. If some or all of the segments are insulated, the user may set  $ISC(J) = 1$  for the appropriate segment numbers J.

```

0001  COMPLEX EP2,EP3,ETA,GAM,Y11,Z11,Z5
0002  COMPLEX EPS,EP1S,EP2S,EP3S,EP4S,EP5S,EP6S,EP7S,EP8S,EP9S,EP10S,EP11S,EP12S,EP13S,EP14S,EP15S,EP16S,EP17S,EP18S,EP19S,EP20S,EP21S,EP22S,EP23S,EP24S,EP25S,EP26S,EP27S,EP28S,EP29S,EP30S,EP31S,EP32S,EP33S,EP34S,EP35S,EP36S,EP37S,EP38S,EP39S,EP40S,EP41S,EP42S,EP43S,EP44S,EP45S,EP46S,EP47S,EP48S,EP49S,EP50S,EP51S,EP52S,EP53S,EP54S,EP55S,EP56S,EP57S,EP58S,EP59S,EP60S,EP61S,EP62S,EP63S,EP64S,EP65S,EP66S,EP67S,EP68S,EP69S,EP70S,EP71S,EP72S,EP73S,EP74S,EP75S,EP76S,EP77S,EP78S,EP79S,EP80S,EP81S,EP82S,EP83S,EP84S,EP85S,EP86S,EP87S,EP88S,EP89S,EP90S,EP91S,EP92S,EP93S,EP94S,EP95S,EP96S,EP97S,EP98S,EP99S,EP100S,EP101S,EP102S,EP103S,EP104S,EP105S,EP106S,EP107S,EP108S,EP109S,EP110S,EP111S,EP112S,EP113S,EP114S,EP115S,EP116S,EP117S,EP118S,EP119S,EP120S,EP121S,EP122S,EP123S,EP124S,EP125S,EP126S,EP127S,EP128S,EP129S,EP130S,EP131S,EP132S,EP133S,EP134S,EP135S,EP136S,EP137S,EP138S,EP139S,EP140S,EP141S,EP142S,EP143S,EP144S,EP145S,EP146S,EP147S,EP148S,EP149S,EP150S,EP151S,EP152S,EP153S,EP154S,EP155S,EP156S,EP157S,EP158S,EP159S,EP160S,EP161S,EP162S,EP163S,EP164S,EP165S,EP166S,EP167S,EP168S,EP169S,EP170S,EP171S,EP172S,EP173S,EP174S,EP175S,EP176S,EP177S,EP178S,EP179S,EP180S,EP181S,EP182S,EP183S,EP184S,EP185S,EP186S,EP187S,EP188S,EP189S,EP190S,EP191S,EP192S,EP193S,EP194S,EP195S,EP196S,EP197S,EP198S,EP199S,EP200S,EP201S,EP202S,EP203S,EP204S,EP205S,EP206S,EP207S,EP208S,EP209S,EP210S,EP211S,EP212S,EP213S,EP214S,EP215S,EP216S,EP217S,EP218S,EP219S,EP220S,EP221S,EP222S,EP223S,EP224S,EP225S,EP226S,EP227S,EP228S,EP229S,EP230S,EP231S,EP232S,EP233S,EP234S,EP235S,EP236S,EP237S,EP238S,EP239S,EP240S,EP241S,EP242S,EP243S,EP244S,EP245S,EP246S,EP247S,EP248S,EP249S,EP250S,EP251S,EP252S,EP253S,EP254S,EP255S,EP256S,EP257S,EP258S,EP259S,EP260S,EP261S,EP262S,EP263S,EP264S,EP265S,EP266S,EP267S,EP268S,EP269S,EP270S,EP271S,EP272S,EP273S,EP274S,EP275S,EP276S,EP277S,EP278S,EP279S,EP280S,EP281S,EP282S,EP283S,EP284S,EP285S,EP286S,EP287S,EP288S,EP289S,EP290S,EP291S,EP292S,EP293S,EP294S,EP295S,EP296S,EP297S,EP298S,EP299S,EP300S,EP301S,EP302S,EP303S,EP304S,EP305S,EP306S,EP307S,EP308S,EP309S,EP310S,EP311S,EP312S,EP313S,EP314S,EP315S,EP316S,EP317S,EP318S,EP319S,EP320S,EP321S,EP322S,EP323S,EP324S,EP325S,EP326S,EP327S,EP328S,EP329S,EP330S,EP331S,EP332S,EP333S,EP334S,EP335S,EP336S,EP337S,EP338S,EP339S,EP340S,EP341S,EP342S,EP343S,EP344S,EP345S,EP346S,EP347S,EP348S,EP349S,EP350S,EP351S,EP352S,EP353S,EP354S,EP355S,EP356S,EP357S,EP358S,EP359S,EP360S,EP361S,EP362S,EP363S,EP364S,EP365S,EP366S,EP367S,EP368S,EP369S,EP370S,EP371S,EP372S,EP373S,EP374S,EP375S,EP376S,EP377S,EP378S,EP379S,EP380S,EP381S,EP382S,EP383S,EP384S,EP385S,EP386S,EP387S,EP388S,EP389S,EP390S,EP391S,EP392S,EP393S,EP394S,EP395S,EP396S,EP397S,EP398S,EP399S,EP400S,EP401S,EP402S,EP403S,EP404S,EP405S,EP406S,EP407S,EP408S,EP409S,EP410S,EP411S,EP412S,EP413S,EP414S,EP415S,EP416S,EP417S,EP418S,EP419S,EP420S,EP421S,EP422S,EP423S,EP424S,EP425S,EP426S,EP427S,EP428S,EP429S,EP430S,EP431S,EP432S,EP433S,EP434S,EP435S,EP436S,EP437S,EP438S,EP439S,EP440S,EP441S,EP442S,EP443S,EP444S,EP445S,EP446S,EP447S,EP448S,EP449S,EP450S,EP451S,EP452S,EP453S,EP454S,EP455S,EP456S,EP457S,EP458S,EP459S,EP460S,EP461S,EP462S,EP463S,EP464S,EP465S,EP466S,EP467S,EP468S,EP469S,EP470S,EP471S,EP472S,EP473S,EP474S,EP475S,EP476S,EP477S,EP478S,EP479S,EP480S,EP481S,EP482S,EP483S,EP484S,EP485S,EP486S,EP487S,EP488S,EP489S,EP490S,EP491S,EP492S,EP493S,EP494S,EP495S,EP496S,EP497S,EP498S,EP499S,EP500S,EP501S,EP502S,EP503S,EP504S,EP505S,EP506S,EP507S,EP508S,EP509S,EP510S,EP511S,EP512S,EP513S,EP514S,EP515S,EP516S,EP517S,EP518S,EP519S,EP520S,EP521S,EP522S,EP523S,EP524S,EP525S,EP526S,EP527S,EP528S,EP529S,EP530S,EP531S,EP532S,EP533S,EP534S,EP535S,EP536S,EP537S,EP538S,EP539S,EP540S,EP541S,EP542S,EP543S,EP544S,EP545S,EP546S,EP547S,EP548S,EP549S,EP550S,EP551S,EP552S,EP553S,EP554S,EP555S,EP556S,EP557S,EP558S,EP559S,EP560S,EP561S,EP562S,EP563S,EP564S,EP565S,EP566S,EP567S,EP568S,EP569S,EP570S,EP571S,EP572S,EP573S,EP574S,EP575S,EP576S,EP577S,EP578S,EP579S,EP580S,EP581S,EP582S,EP583S,EP584S,EP585S,EP586S,EP587S,EP588S,EP589S,EP590S,EP591S,EP592S,EP593S,EP594S,EP595S,EP596S,EP597S,EP598S,EP599S,EP600S,EP601S,EP602S,EP603S,EP604S,EP605S,EP606S,EP607S,EP608S,EP609S,EP610S,EP611S,EP612S,EP613S,EP614S,EP615S,EP616S,EP617S,EP618S,EP619S,EP620S,EP621S,EP622S,EP623S,EP624S,EP625S,EP626S,EP627S,EP628S,EP629S,EP630S,EP631S,EP632S,EP633S,EP634S,EP635S,EP636S,EP637S,EP638S,EP639S,EP640S,EP641S,EP642S,EP643S,EP644S,EP645S,EP646S,EP647S,EP648S,EP649S,EP650S,EP651S,EP652S,EP653S,EP654S,EP655S,EP656S,EP657S,EP658S,EP659S,EP660S,EP661S,EP662S,EP663S,EP664S,EP665S,EP666S,EP667S,EP668S,EP669S,EP670S,EP671S,EP672S,EP673S,EP674S,EP675S,EP676S,EP677S,EP678S,EP679S,EP680S,EP681S,EP682S,EP683S,EP684S,EP685S,EP686S,EP687S,EP688S,EP689S,EP690S,EP691S,EP692S,EP693S,EP694S,EP695S,EP696S,EP697S,EP698S,EP699S,EP700S,EP701S,EP702S,EP703S,EP704S,EP705S,EP706S,EP707S,EP708S,EP709S,EP710S,EP711S,EP712S,EP713S,EP714S,EP715S,EP716S,EP717S,EP718S,EP719S,EP720S,EP721S,EP722S,EP723S,EP724S,EP725S,EP726S,EP727S,EP728S,EP729S,EP730S,EP731S,EP732S,EP733S,EP734S,EP735S,EP736S,EP737S,EP738S,EP739S,EP740S,EP741S,EP742S,EP743S,EP744S,EP745S,EP746S,EP747S,EP748S,EP749S,EP750S,EP751S,EP752S,EP753S,EP754S,EP755S,EP756S,EP757S,EP758S,EP759S,EP760S,EP761S,EP762S,EP763S,EP764S,EP765S,EP766S,EP767S,EP768S,EP769S,EP770S,EP771S,EP772S,EP773S,EP774S,EP775S,EP776S,EP777S,EP778S,EP779S,EP780S,EP781S,EP782S,EP783S,EP784S,EP785S,EP786S,EP787S,EP788S,EP789S,EP790S,EP791S,EP792S,EP793S,EP794S,EP795S,EP796S,EP797S,EP798S,EP799S,EP800S,EP801S,EP802S,EP803S,EP804S,EP805S,EP806S,EP807S,EP808S,EP809S,EP810S,EP811S,EP812S,EP813S,EP814S,EP815S,EP816S,EP817S,EP818S,EP819S,EP820S,EP821S,EP822S,EP823S,EP824S,EP825S,EP826S,EP827S,EP828S,EP829S,EP830S,EP831S,EP832S,EP833S,EP834S,EP835S,EP836S,EP837S,EP838S,EP839S,EP840S,EP841S,EP842S,EP843S,EP844S,EP845S,EP846S,EP847S,EP848S,EP849S,EP850S,EP851S,EP852S,EP853S,EP854S,EP855S,EP856S,EP857S,EP858S,EP859S,EP860S,EP861S,EP862S,EP863S,EP864S,EP865S,EP866S,EP867S,EP868S,EP869S,EP870S,EP871S,EP872S,EP873S,EP874S,EP875S,EP876S,EP877S,EP878S,EP879S,EP880S,EP881S,EP882S,EP883S,EP884S,EP885S,EP886S,EP887S,EP888S,EP889S,EP890S,EP891S,EP892S,EP893S,EP894S,EP895S,EP896S,EP897S,EP898S,EP899S,EP900S,EP901S,EP902S,EP903S,EP904S,EP905S,EP906S,EP907S,EP908S,EP909S,EP910S,EP911S,EP912S,EP913S,EP914S,EP915S,EP916S,EP917S,EP918S,EP919S,EP920S,EP921S,EP922S,EP923S,EP924S,EP925S,EP926S,EP927S,EP928S,EP929S,EP930S,EP931S,EP932S,EP933S,EP934S,EP935S,EP936S,EP937S,EP938S,EP939S,EP940S,EP941S,EP942S,EP943S,EP944S,EP945S,EP946S,EP947S,EP948S,EP949S,EP950S,EP951S,EP952S,EP953S,EP954S,EP955S,EP956S,EP957S,EP958S,EP959S,EP960S,EP961S,EP962S,EP963S,EP964S,EP965S,EP966S,EP967S,EP968S,EP969S,EP970S,EP971S,EP972S,EP973S,EP974S,EP975S,EP976S,EP977S,EP978S,EP979S,EP980S,EP981S,EP982S,EP983S,EP984S,EP985S,EP986S,EP987S,EP988S,EP989S,EP990S,EP991S,EP992S,EP993S,EP994S,EP995S,EP996S,EP997S,EP998S,EP999S,EP1000S,EP1001S,EP1002S,EP1003S,EP1004S,EP1005S,EP1006S,EP1007S,EP1008S,EP1009S,EP1010S,EP1011S,EP1012S,EP1013S,EP1014S,EP1015S,EP1016S,EP1017S,EP1018S,EP1019S,EP1020S,EP1021S,EP1022S,EP1023S,EP1024S,EP1025S,EP1026S,EP1027S,EP1028S,EP1029S,EP1030S,EP1031S,EP1032S,EP1033S,EP1034S,EP1035S,EP1036S,EP1037S,EP1038S,EP1039S,EP1040S,EP1041S,EP1042S,EP1043S,EP1044S,EP1045S,EP1046S,EP1047S,EP1048S,EP1049S,EP1050S,EP1051S,EP1052S,EP1053S,EP1054S,EP1055S,EP1056S,EP1057S,EP1058S,EP1059S,EP1060S,EP1061S,EP1062S,EP1063S,EP1064S,EP1065S,EP1066S,EP1067S,EP1068S,EP1069S,EP1070S,EP1071S,EP1072S,EP1073S,EP1074S,EP1075S,EP1076S,EP1077S,EP1078S,EP1079S,EP1080S,EP1081S,EP1082S,EP1083S,EP1084S,EP1085S,EP1086S,EP1087S,EP1088S,EP1089S,EP1090S,EP1091S,EP1092S,EP1093S,EP1094S,EP1095S,EP1096S,EP1097S,EP1098S,EP1099S,EP1100S,EP1101S,EP1102S,EP1103S,EP1104S,EP1105S,EP1106S,EP1107S,EP1108S,EP1109S,EP1110S,EP1111S,EP1112S,EP1113S,EP1114S,EP1115S,EP1116S,EP1117S,EP1118S,EP1119S,EP1120S,EP1121S,EP1122S,EP1123S,EP1124S,EP1125S,EP1126S,EP1127S,EP1128S,EP1129S,EP1130S,EP1131S,EP1132S,EP1133S,EP1134S,EP1135S,EP1136S,EP1137S,EP1138S,EP1139S,EP1140S,EP1141S,EP1142S,EP1143S,EP1144S,EP1145S,EP1146S,EP1147S,EP1148S,EP1149S,EP1150S,EP1151S,EP1152S,EP1153S,EP1154S,EP1155S,EP1156S,EP1157S,EP1158S,EP1159S,EP1160S,EP1161S,EP1162S,EP1163S,EP1164S,EP1165S,EP1166S,EP1167S,EP1168S,EP1169S,EP1170S,EP1171S,EP1172S,EP1173S,EP1174S,EP1175S,EP1176S,EP1177S,EP1178S,EP1179S,EP1180S,EP1181S,EP1182S,EP1183S,EP1184S,EP1185S,EP1186S,EP1187S,EP1188S,EP1189S,EP1190S,EP1191S,EP1192S,EP1193S,EP1194S,EP1195S,EP1196S,EP1197S,EP1198S,EP1199S,EP1200S,EP1201S,EP1202S,EP1203S,EP1204S,EP1205S,EP1206S,EP1207S,EP1208S,EP1209S,EP1210S,EP1211S,EP1212S,EP1213S,EP1214S,EP1215S,EP1216S,EP1217S,EP1218S,EP1219S,EP1220S,EP1221S,EP1222S,EP1223S,EP1224S,EP1225S,EP1226S,EP1227S,EP1228S,EP1229S,EP1230S,EP1231S,EP1232S,EP1233S,EP1234S,EP1235S,EP1236S,EP1237S,EP1238S,EP1239S,EP1240S,EP1241S,EP1242S,EP1243S,EP1244S,EP1245S,EP1246S,EP1247S,EP1248S,EP1249S,EP1250S,EP1251S,EP1252S,EP1253S,EP1254S,EP1255S,EP1256S,EP1257S,EP1258S,EP1259S,EP1260S,EP1261S,EP1262S,EP1263S,EP1264S,EP1265S,EP1266S,EP1267S,EP1268S,EP1269S,EP1270S,EP1271S,EP1272S,EP1273S,EP1274S,EP1275S,EP1276S,EP1277S,EP1278S,EP1279S,EP1280S,EP1281S,EP1282S,EP1283S,EP1284S,EP1285S,EP1286S,EP1287S,EP1288S,EP1289S,EP1290S,EP1291S,EP1292S,EP1293S,EP1294S,EP1295S,EP1296S,EP1297S,EP1298S,EP1299S,EP1300S,EP1301S,EP1302S,EP1303S,EP1304S,EP1305S,EP1306S,EP1307S,EP1308S,EP1309S,EP1310S,EP1311S,EP1312S,EP1313S,EP1314S,EP1315S,EP1316S,EP1317S,EP1318S,EP1319S,EP1320S,EP1321S,EP1322S,EP1323S,EP1324S,EP1325S,EP1326S,EP1327S,EP1328S,EP1329S,EP1330S,EP1331S,EP1332S,EP1333S,EP1334S,EP1335S,EP1336S,EP1337S,EP1338S,EP1339S,EP1340S,EP1341S,EP1342S,EP1343S,EP1344S,EP1345S,EP1346S,EP1347S,EP1348S,EP1349S,EP1350S,EP1351S,EP1352S,EP1353S,EP1354S,EP1355S,EP1356S,EP1357S,EP1358S,EP1359S,EP1360S,EP1361S,EP1362S,EP1363S,EP1364S,EP1365S,EP1366S,EP1367S,EP1368S,EP1369S,EP1370S,EP1371S,EP1372S,EP1373S,EP1374S,EP1375S,EP1376S,EP1377S,EP1378S,EP1379S,EP1380S,EP1381S,EP1382S,EP1383S,EP1384S,EP1385S,EP1386S,EP1387S,EP1388S,EP1389S,EP1390S,EP1391S,EP1392S,EP1393S,EP1394S,EP1395S,EP1396S,EP1397S,EP1398S,EP1399S,EP1400S,EP1401S,EP1402S,EP1403S,EP1404S,EP1405S,EP1406S,EP1407S,EP1408S,EP1409S,EP1410S,EP1411S,EP1412S,EP1413S,EP1414S,EP1415S,EP1416S,EP1417S,EP1418S,EP1419S,EP1420S,EP1421S,EP1422S,EP1423S,EP1424S,EP1425S,EP1426S,EP1427S,EP1428S,EP1429S,EP1430S,EP1431S,EP1432S,EP1433S,EP1434S,EP1435S,EP1436S,EP1437S,EP1438S,EP1439S,EP1440S,EP1441S,EP1442S,EP1443S,EP1444S,EP1445S,EP1446S,EP1447S,EP1448S,EP1449S,EP1450S,EP1451S,EP1452S,EP1453S,EP1454S,EP1455S,EP1456S,EP1457S,EP1458S,EP1459S,EP1460S,EP1461S,EP1462S,EP1463S,EP1464S,EP1465S,EP1466S,EP1467S,EP1468S,EP1469S,EP1470S,EP1471S,EP1472S,EP1473S,EP1474S,EP1475S,EP1476S,EP1477S,EP1478S,EP1479S,EP1480S,EP1481S,EP1482S,EP1483S,EP1484S,EP1485S,EP1486S,EP1487S,EP1488S,EP1489S,EP1490S,EP1491S,EP1492S,EP1493S,EP1494S,EP1495S,EP1496S,EP1497S,EP1498S,EP1499S,EP1500S,EP1501S,EP1502S,EP1503S,EP1504S,EP1505S,EP1506S,EP1507S,EP1508S,EP1509S,EP1510S,EP1511S,EP1512S,EP1513S,EP1514S,EP1515S,EP1516S,EP1517S,EP1518S,EP1519S,EP1520S,EP1521S,EP1522S,EP1523S,EP1524S,EP1525S,EP1526S,EP1527S,EP1528S,EP1529S,EP1530S,EP1531S,EP1532S,EP1533S,EP1534S,EP1535S,EP1536S,EP1537S,EP1538S,EP1539S,EP1540S,EP1541S,EP1542S,EP1543S,EP1544S,EP1545S,EP1546S,EP1547S,EP1548S,EP1549S,EP1550S,EP1551S,EP1552S,EP1553S,EP1554S,EP1555S,EP1556S,EP1557S,EP1558S,EP1559S,EP1560S,EP1561S,EP1562S,EP1563S,EP1564S,EP1565S,EP1566S,EP1567S,EP1568S,EP1569S,EP1570S,EP1571S,EP1572S,EP1573S,EP1574S,EP1575S,EP1576S,EP1577S,EP1578S,EP1579S,EP1580S,EP1581S,EP1582S,EP1583S,EP1584S,EP1585S,EP1586S,EP1587S,EP1588S,EP1589S,EP1590S,EP1591S,EP1592S,EP1593S,EP1594S,EP1595S,EP1596S,EP1597S,EP1598S,EP1599S,EP1600S,EP1601S,EP1602S,EP1603S,EP1604S,EP1605S,EP1606S,EP1607S,EP1608S,EP1609S,EP1610S,EP1611S,EP1612S,EP1613S,EP1614S,EP1615S,EP1616S,EP1617S,EP1618S,EP1619S,EP1620S,EP1621S,EP1622S,EP1623S,EP1624S,EP1625S,EP1626S,EP1627S,EP1628S,EP1629S,EP1630S,EP1631S,EP1632S,EP1633S,EP1634S,EP1635S,EP1636S,EP1637S,EP1638S,EP1639S,EP1640S,EP1641S,EP1642S,EP1643S,EP1644S,EP1645S,EP1646S,EP1647S,EP1648S,EP1649S,EP1650S,EP1651S,EP1652S,EP1653S,EP1654S,EP1655S,EP1656S,EP1657S,EP1658S,EP1659S,EP1660S,EP1661S,EP1662S,EP1663S,EP1664S,EP1665S,EP1666S,EP1667S,EP1668S,EP1669S,EP1670S,EP1671S,EP1672S,EP1673S,EP1674S,EP1675S,EP1676S,EP1677S,EP1678S,EP1679S,EP1680S,EP1681S,EP1682S,EP1683S,EP1684S,EP1685S,EP1686S,EP1687S,EP1688S,EP1689S,EP1690S,EP1691S,EP1692S,EP1693S,EP1694S,EP1695S,EP1696S,EP1697S,EP1698S,EP1699S,EP1700S,EP1701S,EP1702S,EP1703S,EP1704S,EP1705S,EP1706S,EP1707S,EP1708S,EP1709S,EP1710S,EP1711S,EP1712S,EP1713S,EP1714S,EP1715S,EP1716S,EP1717S,EP1718S,EP1719S,EP1720S,EP1721S,EP1722S,EP1723S,EP1724S,EP1725S,EP1726S,EP1727S,EP1728S,EP1729S,EP1730S,EP1731S,EP1732S,EP1733S,EP1734S,EP1735S,EP1736S,EP1737S,EP1738S,EP1739S,EP1740S,EP1741S,EP1742S,EP1743S,EP1744S,EP1745S,EP1746S,EP1747S,EP1748S,EP1749S,EP1750S,EP1751S,EP1752S,EP1753S,EP1754S,EP1755S,EP1756S,EP1757S,EP1758S,EP1759S,EP1760S,EP1761S,EP1762S,EP1763S,EP1764S,EP1765S,EP1766S,EP1767S,EP1768S,EP1769S,EP1770S,EP1771S,EP1772S,EP1773S,EP1774S,EP1775S,EP1776S,EP1777S,EP1778S,EP1779S,EP1780S,EP1781S,EP1782S,EP1783
```

```

CALL GANT1(1A,1B,1NM,1MR,11,12,13,112,1A,1B,MD,N,ND,NM,AM
2,C,CJ,CG,CM,D,EFF,GAM,GG,CGO,SGO,YIG,Y11,Z11,ZLD,ZS)
WRITE(6,3)EFF,GG,Z11
200 IF (1NEAR.LE.0)GO TO 300
CALL GNFID(1A,1B,1NM,11,12,13,MD,N,ND,NM,AM,CGO,SGO,ETA,GAM
2,C,CJ,D,X,Y,Z,XP,YP,ZP,EX,EY,EZ)
WRITE(6,3)XP,YP,ZP
WRITE(6,6)EX,EY,EZ
300 IF (1IGAIN.LE.0)GO TO 400
INC=0
PH=PHA
TH=THA
CALL GFFID(1A,1B,1NC,1NM,1MR,11,12,13,112,MD,N,ND,NM,AM
2,ACSP,ACST,C,CGO,CG,CJ,CM,D,ECSP,ECST,EP,ET,EPP,ETT,EPPS,EPTS
3,ETPS,ETTS,GG,GPP,GTT,PH,SGO,SCSP,SCST,SPPM,STPM,STTM,TH
4,X,Y,Z,ZLD,ZS,ETA,GAM)
WRITE(6,3)PH,TH,GPP,GTT
400 IF (1SCAT.LE.0)GO TO 600
INC=1
PH=PHI
TH=THI
CALL GFFID(1A,1B,1NC,1NM,1MR,11,12,13,112,MD,N,ND,NM,AM
2,ACSP,ACST,C,CGO,CG,CJ,CM,D,ECSP,ECST,EP,ET,EPP,ETT,EPPS,EPTS
3,ETPS,ETTS,GG,GPP,GTT,PH,SGO,SCSP,SCST,SPPM,STPM,STTM,TH
4,X,Y,Z,ZLD,ZS,ETA,GAM)
WRITE(6,6)PH,TH,GPP,GTT,STPM,STTM
WRITE(6,6)ACSP,ACST,ECSP,ECST,SCSP,SCST
500 IF (1BISC.LE.0)GO TO 600
INC=2
PH=PHS
TH=THS
CALL GFFID(1A,1B,1NC,1NM,1MR,11,12,13,112,MD,N,ND,NM,AM
2,ACSP,ACST,C,CGO,CG,CJ,CM,D,ECSP,ECST,EP,ET,EPP,ETT,EPPS,EPTS
3,ETPS,ETTS,GG,GPP,GTT,PH,SGO,SCSP,SCST,SPPM,STPM,STTM,TH
4,X,Y,Z,ZLD,ZS,ETA,GAM)
WRITE(6,6)PH,TH,GPP,GTT,STPM,STTM
600 CONTINUE
800 CALL EXIT
END

```

Fig. 1b. The thin-wire computer program.

The first READ statement inputs the following parameters for the dielectric insulation:

BM	outer radius in meters
ER2	dielectric constant relative to free space
SIG2	conductivity in mhos per meter
TD2	loss tangent

The program will use SIG2 or TD2 but not both. The user determines which one will be used by assigning the other a negative value. For an uninsulated wire structure, the program will not use any of the data from the first READ statement.

The second READ statement inputs the following parameters for the wire and the exterior medium:

AM	wire radius in meters
CM	wire conductivity in megamhos per meter
ER3	dielectric constant relative to free space
SIG3	conductivity in mhos per meter
TD3	loss tangent

The parameters ER3, SIG3 and TD3 are those of the homogeneous ambient medium. Again, the program will use SIG3 or TD3 but not both.

The third READ statement inputs the following data:

IBISC	indicator for bistatic scattering calculations
IGAIN	indicator for antenna gain calculations
INEAR	indicator for near-zone field calculations
ISCAT	indicator for backscatter calculations
IMR	indicator for writeout of current distributions
NGEN	indicator for antenna calculations
NM	number of monopoles (segments)
NP	number of points

For each indicator, a positive value means the calculation or writeout is desired while a zero or negative value means it is not desired.

The fourth READ statement inputs the following data:

FM	frequency in megahertz
PHA,THA	far-field angle for antenna gain
PHI,THI	incidence angle for plane-wave scattering
PHS,THS	scattering angle for bistatic scattering

The above angles are given in degrees, and they denote values of the angular coordinates in the spherical system ( $r, \theta, \phi$ ) widely used in antenna and scattering literature.



The fifth READ statement (in the DO LOOP ending with statement 22) inputs the endpoints IA(J) and IB(J) of segment J. Thus, IA and IB are the index numbers of the two points which are joined by segment J.

The sixth READ statement (in the DO LOOP ending with statement 40) inputs the coordinates X(I), Y(I) and Z(I) of point I in meters. The seventh and last READ statement inputs the coordinates XP, YP and ZP (in meters) of the observation point for near-zone field calculations.

Some of the quantities used in the program are defined as follows:

FHZ	frequency in Hertz
OMEGA	angular frequency
EP2	complex permittivity of insulation
EP3	complex permittivity of ambient medium
ETA	intrinsic impedance of ambient medium
GAM	intrinsic propagation constant of ambient medium
ZS	surface impedance of wire
ZLD	load impedances

For an uninsulated wire with perfect conductivity, one may specify complex values for ETA and GAM and delete the following input data and calculations: BM, ER2, SIG2, TD2, ER3, SIG3, TD3, FMC, FHZ, OMEGA, EP2 and EP3.

After reading the input data, the program calls subroutine SORT. This subroutine defines a set of dipole modes on the wire structure. N denotes the total number of dipole modes, the number of simultaneous linear equations, and the size of the impedance matrix  $Z_{ij}$ . Since this matrix is symmetric, only the upper-right triangular portion (including the entire principal diagonal) is calculated and stored in C(K). SORT calculates N, but the user may predict N as follows to reserve adequate storage. If m wire segments intersect at a point, this point is defined as a junction of order m and degree  $n = m - 1$ . There will be n dipole modes with terminals at this junction. N is determined by summing the degrees of all the junctions. For an example, an endpoint of a dipole is a junction of order  $m = 1$  and degree  $n = 0$ . The vertex of a V dipole is a junction of order 2 and degree 1. NP denotes the number of points on the wire structure, and each of these points is considered to be a junction.

Mode I is a two-segment V dipole with a sinusoidal current distributed over the intersecting segments JA(I) and JB(I). The dipole has endpoints I1(I) and I3(I) and terminals at I2(I). The reference direction for positive current on dipole I is from I1 to I2 to I3.

A wire segment may be shared by as many as four dipole modes, or as few as one. In the output of subroutine SORT, ND(J) denotes the number of dipoles sharing segment J. The extreme values of ND(J) are MAX and MIN. If MIN is less than one, the wire structure has an unconnected segment and the computation is aborted. (An isolated wire

must have at least two segments and three points.) If N exceeds ICJ, the dimensions are inadequate and the run is aborted.

INT specifies the number of intervals for calculating the elements in the impedance matrix with Simpson's-r rule integration. A large value for INT improves the accuracy at the expense of greater execution time. For most problems a suitable combination of speed and accuracy is obtained with INT = 4. A larger value is recommended if one wire passes close to another as in the helix or the multilum loop. If in doubt, one may set INT = 0 to choose the rigorous closed-form impedance expressions in terms of exponential integrals.

The DO LOOP ending with statement 60 sets all the lumped load impedances and generator voltages to zero. If the wire structure has lumped loads, one may insert a READ command after statement 60 to input a list of complex load impedances ZLD(J). For a wire antenna with just one generator, the program inserts a unit voltage generator with  $VG(NGEN) = (1,0,0)$ . If the antenna or array has several generators, one may insert a READ command after statement 60 to input a list of complex voltages VG(J).

Generators or lumped loads may be inserted at either end or both ends of segment J. First consider a load impedance inserted in the middle of segment J. Now slide the load along the segment and let it approach the endpoint IA(J). This load is represented by ZLD(J). Next insert another load in segment J and slide it to approach the endpoint IB(J). This load is designated ZLD(JJ) where JJ = J + NM. The same convention is employed for the voltage generators VG(J) and VG(JJ). A generator voltage VG(J) is considered positive if it tends to force a current flow in the direction from IA(J) to IB(J).

Subroutine SGANT calculates the elements of the impedance matrix  $Z_{ij}$  and stores them in C(K) where  $K = (I-1)*N - (I+1 - I)/2 + J$ . This subroutine will set N = 0 and the run will abort if the wire radius is zero or negative, the shortest segment length is less than the wire diameter, the wire radius is electrically large, or the longest segment is too long.

Subroutine GANTI considers the thin-wire structure as an antenna and solves for the current distribution CG(J), radiation efficiency EFF, time-average power input GG and complex power input Y11. In the current distribution, CG(J) is the current on segment J as one approaches the endpoint IA(J) and CG(JJ) is the current at the other end IB(J). The reference direction for positive current is from IA to IB. Thus, the conventions are the same for the branch currents CG and the branch voltages VG.

If the antenna has only one voltage generator with  $VG(NGEN) = (1,0,0)$ , then Y11 is the antenna admittance and Z11 is the impedance.

The radiation efficiency EFF is calculated from the time-average power input to the antenna and the time-average power dissipated in the wire and the lumped loads. If the antenna is insulated, the power dissipated in the insulation is neglected. If the wire has perfect conductivity and the loads are purely reactive, the calculated efficiency will be 100 per cent.

The near-field subroutine GNFLD calculates the electric field intensity (EX,EY,EZ) at the observation point (XP,YP,ZP). In the calling parameters, CJ denotes the current distribution on the wire. (The loop currents are stored in CJ(I) and the branch currents in CG(J)). Thus, the currents must be calculated before GNFLD is called. Fig. 1 illustrates the use of GNFLD to calculate the near-zone field in an antenna problem. This subroutine can be called again just above statement 500 to calculate the near-zone scattered field for a wire target. In the calling parameters, CJ is replaced with EP or ET to obtain the near-zone field with a phi-polarized or theta-polarized incident plane wave. Reference 1 describes the more sophisticated techniques required when the observation point is extremely close to the wire structure.

The far-field subroutine GFFLD calculates antenna gain if INC = 0, backscattering if INC = 1, and bistatic scattering if INC = 2. If INC = 0, PH and TH denote the spherical coordinates  $\phi$  and  $\theta$  of the distant observation point and the output from GFFLD is defined as follows. EPPS and ETTIS denote the phi-polarized and theta-polarized components of the electric field intensity. For example,

$$(1) \quad EPPS = r e^{j\gamma r} E_{\phi}$$

where  $r$  is the distance from the origin to the observation point. GPP and GTT denote the power gains associated with the phi and theta polarizations. Appendix 14 defines GPP and GTT more precisely.

If INC = 1, PH and TH denote the incidence angles  $\phi_i$  and  $\theta_i$ . These are also the spherical coordinates of the distant source. In this backscattering situation, the output data from GFFLD are defined as follows:

ACSP,ACST	absorption cross sections for $\phi$ and $\theta$ polarizations
ECSP,ECAST	extinction cross sections for $\phi$ and $\theta$ polarizations
EP,ET	loop currents induced by $\phi$ and $\theta$ polarized waves
EPPS	scattered electric field $E_{\phi\phi}$
EPTS	scattered electric field $E_{\theta\phi}$
ETPS	scattered electric field $E_{\phi\theta}$
ETTS	scattered electric field $E_{\theta\theta}$
SCSP,SCST	scattering cross sections for $\phi$ and $\theta$ polarizations
SPPM	echo area $\sigma_{\phi\phi}$

SPTM	echo area $\sigma_{\theta\theta}$
STPM	echo area $\sigma_{\phi\phi}$
STTM	echo area $\sigma_{\theta\theta}$

The echo areas are given in square meters. For the doubly-subscripted quantities such as  $E_{\phi\phi}$  and  $\sigma_{\phi\phi}$ , the first and second subscripts specify the polarizations of the incident and scattered waves, respectively. The complex numbers EPPS, EPTS, ETPS and ETTIS are the elements of the polarization scattering matrix.

If INC = 2, PH and TH denote the scattering angles  $\phi_s$  and  $\theta_s$ . These are the spherical coordinates of the distant observer. In this bistatic scattering situation, the only outputs from GFFLD are the polarization scattering matrix and the echo areas.

To obtain antenna patterns, backscattering patterns or bistatic patterns, one may insert DO LOOPS in the program to increment the angles PH and TH. The DO LOOP will begin just above the call to GFFLD and terminate just below this call. To obtain the near-zone field distribution along a given probing path, one may insert a DO LOOP beginning just above the call to GNFLD and terminating just below this call.

When the calculations have been completed for one problem, one may GO TO a point just above CALL GANT1 if only the generator voltages are to be changed. One may GO TO a point just below CALL SORT if there is a change in the wire radius or conductivity, the insulation, ambient medium, frequency, load impedances or the coordinates (X,Y,Z). If there is a change in NM, NP, IA or IB, one should GO TO a point above CALL SORT.

Consider an array of three center-fed dipoles, and suppose we desire the  $3 \times 3$  admittance matrix for the array. Let each dipole be divided into four segments with segments 1 through 4 on dipole 1, 5 through 8 on dipole 2 and 9 through 12 on dipole 3. The three-port admittance matrix can be obtained by inserting a DO LOOP beginning just above CALL GANT1 and terminating just below this call. GANT1 will be called three times with all the voltages VG set to zero except for a single one-volt generator. On the first, second and third calls, let NGEN = 3, 7 and 11 to represent a generator at the center of dipole 1, 2 and 3, respectively. After the first call, set Y11 = CG(3), Y12 = CG(7) and Y13 = CG(11). Set Y22 = CG(7) and Y23 = CG(11) after the second call and Y33 = CG(11) after the third call.

For extremely small antennas, quasi-static or double-precision subroutines are required.

The wire radius must exceed zero, but there is no difficulty with small radii. If the radius exceeds 0.007 $\lambda$ , the thin-wire assumptions are questionable and the accuracy and convergence deteriorate. The length ratio of the longest and shortest segments should not exceed 100. It is



assumed that the wire length exceeds the wire diameter by a factor of at least 30. We are not aware of any lower limit on the segment length, however.

If a wire is bent sharply to form a small acute angle (less than 30 degrees), the thin-wire model is questionable. It is assumed that the wire conductivity greatly exceeds the conductivity of the ambient medium. For insulated wires, the dielectric layer is assumed to be electrically thin.

For each thin-wire problem, calculations should be repeated several times with the wire divided progressively into shorter segments. There is no assurance of accuracy until the output data converge. For a moderately thick wire (with radius  $a = 0.007 \lambda$  or larger), the susceptance may diverge with the delta-gap model. This difficulty may be alleviated or eliminated with the magnetic-frill model and the techniques of Imbriate and Ingerson [2].

Tables 1, 2 and 3 list input and output data for three simple examples of uninsulated wire structures. Each table includes a sketch of the wire configuration with labels to indicate the numbering system for the points and segments. In these examples there are no lumped loads.

In the sinusoidal-reaction formulation, a basic function is the mutual impedance between two sinusoidal filamentary electric dipoles. One dipole is a test source located on the axis of the wire structure, and the other is an expansion mode on the wire surface. In view of the importance of this mutual impedance, short tables are presented next for a few simple cases. The data can be reproduced with the program in Fig. 1 with appropriate input data for uninsulated wires with perfect conductivity and no lumped loads in free space. The data were obtained with the closed-form expressions (INT = 0) by writing out the quantities C(K) just below the call to subroutine SGANT. Double precision was used for these calculations.

Table 4 lists the self impedance of a two-segment sinusoidal Y dipole with radius  $a = 0.001 \lambda$ . Subroutine SGANT calculates this quantity by setting up one filamentary dipole on the wire axis and another identical dipole on the wire surface. These dipoles lie in parallel planes separated by a distance equal to the wire radius.

In Table 5, dipoles 1 and 2 have terminals at vertices 1 and 2, respectively, and they share the middle segment. Again these dipoles lie in parallel planes separated by a distance equal to the wire radius. For a one-turn planar polygon wire loop, subroutine SGANT would generate the data in Table 4 for the diagonal elements  $Z_{ij}$  and the data in Table 5 for the next elements.

TABLE 1  
Input and Output Data for Straight Wire

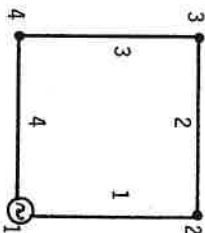
Input Data		Output Data	
0.002	2.56	-1.0	0.0005
0.001	1.00	1.0	-1.0
1	1	1	1
300.	0.	90.	0.
1	2	0.	0.
2	3	0.	0.
3	4	0.	0.
4	5	0.	0.
0.	0.	-0.250	-0.125
0.	0.	0.	0.
0.	0.	0.	0.
0.	0.	0.125	0.250
0.	0.	0.250	1.
1.	1.	1.	1.



TABLE 2  
Input and Output Data for Square Loop

Input Data		Output Data	
98.18	0.0095	82.97	43.26
-0.091	0.080	-0.091	0.080
0.0	90.0	0.0	1.615
0.0	90.0	0.0	0.0
0.0	0.0069	0.0	0.377
45.0	45.0	0.0	0.0
		0.0	0.224
		0.0	-0.096
		0.0	0.608
		0.0	0.370
		0.0	0.239

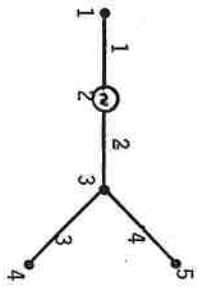
Input Data		Output Data	
0.002	2.56	-1.0	0.0005
0.001	1.0	1.0	-1.0
1	1	1	1
300.	0.0	90.0	0.0
1	2	0.0	0.0
2	3	0.0	0.0
3	4	0.0	0.0
4	1	0.05	0.05
0.05	0.05	0.05	0.0
-0.05	0.05	0.05	0.0
-0.05	-0.05	0.0	0.0
1.0	1.0	1.0	1.0



Input Data		Output Data	
73.10	.243E-4	62.94	1609.8
-.0078	.0027	.0057	.0029
0.0	90.0	.8066	.0
0.0	90.0	.0002	.0
-126E-4	0.0	.936E-4	.0
45.0	45.0	.106E-3	.265E-4
		.0	.810E-4
		.0	.0
		.0	.0
		.0	.0

TABLE 3  
Input and Output Data for V Antenna

Input Data	2.56	-1.0	0.0005	0.0	2	4	5
0.002	1.0	1.0	-1.0	0	90.0	45.	45.
0.001	1	1	1	0	90.0	45.	45.
300.	0.0	90.0	0.0	90.0	45.	45.	45.
1	2	3	4	5	6	7	8
2	3	4	5	6	7	8	9
3	4	5	6	7	8	9	10
0.0	-0.30	0.0	0.0	0.0	0.0	0.0	0.0
0.0	-0.15	0.0	0.0	0.0	0.0	0.0	0.0
0.0	0.0	0.0	0.0	0.0	0.0	0.0	0.0
0.1	0.1	0.0	0.0	0.0	0.0	0.0	0.0
-0.1	0.1	0.0	0.0	0.0	0.0	0.0	0.0
1.0	1.0	1.0	1.0	1.0	1.0	1.0	1.0



Output Data	0.013	75.53	-0.572	-0.126	0.070
97.88	0.081	0.260	-0.064	0.0	0.0
-124	90.0	1.535	0.0	0.0	0.0
0.0	90.0	0.748	0.0	0.0	0.0
0.0	0.0	0.487	0.0	0.477	0.0
0.0103	0.0	0.360	0.170	0.0	0.0
45.0	45.0	0.360	0.170	0.0	0.0

TABLE 4

Self Impedance of Two-Segment V Dipole Shown in Fig. 2  
Radius:  $a = 0.001\lambda$

$\psi$	$h = 0.10\lambda$	$h = 0.15\lambda$	$h = 0.20\lambda$	$h = 0.25\lambda$
30°	0.59 - j 481	1.4 - j 314	3.1 - j 186	6.1 - j 61
60	2.15 - j 547	5.3 - j 337	11.0 - j 177	21.3 - j 21
90	4.22 - j 572	10.4 - j 340	21.1 - j 163	40.0 - j 9
120	6.31 - j 583	15.3 - j 338	30.9 - j 151	57.7 - j 28
150	7.81 - j 587	18.9 - j 335	37.7 - j 144	69.3 - j 39
180	8.33 - j 589	20.1 - j 335	39.9 - j 142	73.1 - j 42

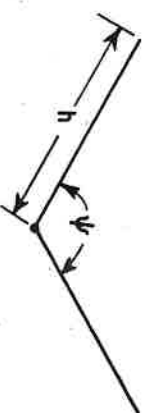


Fig. 2. Symmetric center-fed V dipole.

TABLE 5  
Mutual Impedance Between Overlapping V Dipoles in Fig. 3  
Radius:  $a = 0.001\lambda$

$\psi$	$h = 0.10\lambda$	$h = 0.15\lambda$	$h = 0.20\lambda$	$h = 0.25\lambda$
60°	-0.96 + j 338	-2.08 + j 285	-3.45 + j 275	-4.8 + j 298
90	0.19 + j 322	1.03 + j 276	3.57 + j 271	10.1 + j 297
120	3.29 + j 336	8.40 + j 290	17.86 + j 285	35.3 + j 309
150	6.61 + j 346	15.61 + j 299	30.00 + j 291	52.9 + j 309
180	8.01 + j 349	18.47 + j 301	34.35 + j 292	58.2 + j 308

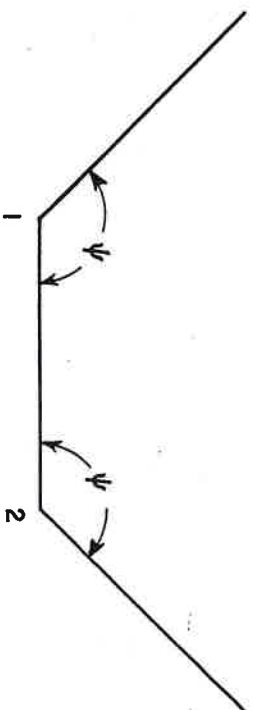


Fig. 3. Overlapping V dipoles share the middle segment.

Tables 6, 7, and 8 list the mutual impedance for other configurations. In all these tables, the data apply to two-segment center-fed sinusoidal dipoles with identical segment lengths  $h$ .



TABLE 6  
Mutual Impedance Between Overlapping V Dipoles in Fig. 4  
Radius:  $a = 0.001\lambda$

$\alpha$	$h = 0.10\lambda$	$h = 0.15\lambda$	$h = 0.20\lambda$	$h = 0.25\lambda$
30°	6.74 - j 314	16.24 - j 167	32.17 - j 56	58.7 + j 49.6
60	3.16 - j 291	7.68 - j 169	15.47 - j 76	28.8 + j 14.2
90	0.06 - j 278	0.31 - j 172	1.15 - j 92	3.5 - j 12.2
120	-1.01 - j 256	-2.39 - j 168	-4.47 - j 101	-7.6 - j 35.5
150	-0.48 - j 207	-1.20 - j 146	-2.40 - j 98	-4.5 - j 50.7

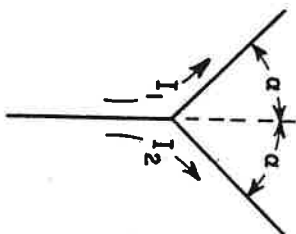


Fig. 4. Overlapping V dipoles share the bottom segment in a planar Y configuration.

TABLE 7  
Mutual Impedance Between the Coplanar-Skew Linear Dipoles in Fig. 5  
Displacement:  $d = \lambda$

$\theta$	$h = 0.10\lambda$	$h = 0.15\lambda$	$h = 0.20\lambda$	$h = 0.25\lambda$
0°	0.337 + j 1.952	0.880 + j 4.759	1.932 + j 9.547	4.011 + j 17.7
15	0.322 + j 1.884	0.831 + j 4.585	1.799 + j 9.180	3.671 + j 17.0
30	0.281 + j 1.684	0.700 + j 4.082	1.448 + j 8.128	2.800 + j 15.0
45	0.220 + j 1.369	0.521 + j 3.301	1.000 + j 6.519	1.745 + j 11.9
60	0.149 + j 0.964	0.333 + j 2.310	0.579 + j 4.524	0.860 + j 8.1
75	0.075 + j 0.497	0.159 + j 1.187	0.252 + j 2.308	0.305 + j 4.1
90	0.0 + j 0.0	0.0 + j 0.0	0.0 + j 0.0	0.0 + j 0.0

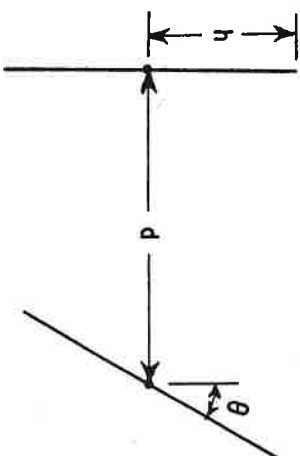


Fig. 5. Center-fed coplanar-skew linear dipoles.

TABLE 8  
Mutual Impedance Between the Nonplanar-Skew Linear Dipoles in Fig. 6  
Displacement:  $d = \lambda$

$\phi$	$h = 0.10\lambda$	$h = 0.15\lambda$	$h = 0.20\lambda$	$h = 0.25\lambda$
0°	0.337 + j 1.952	0.880 + j 4.759	1.932 + j 9.547	4.011 + j 17.74
15	0.326 + j 1.886	0.850 + j 4.596	1.867 + j 9.222	3.877 + j 17.14
30	0.292 + j 1.691	0.762 + j 4.121	1.675 + j 8.259	3.482 + j 15.37
45	0.238 + j 1.380	0.622 + j 3.365	1.369 + j 6.752	2.850 + j 12.55
60	0.169 + j 0.976	0.440 + j 2.380	0.969 + j 4.775	2.020 + j 8.88
75	0.087 + j 0.505	0.228 + j 1.232	0.502 + j 2.472	1.047 + j 4.60
90	0.0 + j 0.0	0.0 + j 0.0	0.0 + j 0.0	0.0 + j 0.0

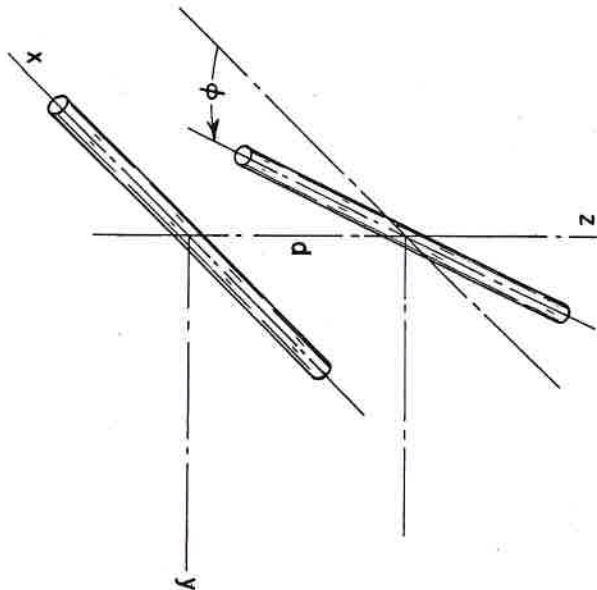


Fig. 6. Center-fed nonplanar-skew linear dipoles.

### III. SUMMARY

This report presents the sinusoidal-reaction computer program for thin-wire antennas and scatterers, instructions for the user, typical input and output data and mutual-impedance tables for sinusoidal dipoles. Appendices list the computer subroutines and explain their functions.

## REFERENCES

1. Richmond, J.H., "Radiation and scattering by thin-wire structures in the complex frequency domain," Report 2902-10, July, 1973, The Ohio State University ElectroScience Laboratory, Department of Electrical Engineering, prepared under Grant NGL 36-008-138 for National Aeronautics and Space Administration, Langley Research Center. (Available as NASA CR-2396, 1974.)
2. Imbriale, W.A., and Ingerson, P.G., "On numerical convergence of moment solutions of moderately thick wire antennas using sinusoidal basis functions," IEEE Trans., Vol. AP-21, May 1973, pp. 363-366.
3. Abramowitz, M., and Stegun, I.A., "Handbook of mathematical functions with formulas, graphs, and mathematical tables," National Bureau of Standards, Applied Mathematics Series AMS-55, 1964, Chapter 5.
4. Faddeev, D.K., and Faddeeva, V.N., Computational Methods of Linear Algebra, W. H. Freeman and Company, San Francisco, 1963, pp. 144-147.

## APPENDIX 1. Subroutine SORT

Subroutine SORT, listed in Fig. 7, defines a set of dipole mode currents on the wire structure. The input data IA, IB, NM, NP, ICJ and INM have been defined already. The output data are defined as follows

N	total number of dipole modes
I1(I)	endpoint of dipole I
I2(I)	terminal point of dipole I
I3(I)	endpoint of dipole I
JA(I)	first segment of dipole I
JB(I)	second segment of dipole I
MD(J,K)	list of dipoles sharing segment J
ND(J)	total number of dipoles sharing segment J
MAX, MIN	extreme values of ND(J)

At completion of the DO LOOP ending with statement 20, NJK denotes the number of segments intersecting at point K, and JSP is a list of these segments. In the DO LOOP ending with statement 22, the computer sets up the appropriate number MOD of dipoles modes with terminals at point K.

## APPENDIX 2. Subroutine SGANT

Subroutine SGANT, listed in Fig. 8, calculates the mutual impedances  $Z_{ij}$  and stores them in C(K). The input data for SGANT have been defined already. The output data are defined as follows:

C(K)	open-circuit impedance matrix
CGD(J)	cosh rd for segment J
SGD(J)	sinh rd for segment J
D(J)	length of segment J
ZS	surface impedance of the wire

The surface impedance is calculated just above statement 12.  $B_0 I$  denotes  $J_0/j_1$  where  $J_0$  and  $J_1$  are the Bessel functions of order zero and one with complex argument ZARG. It is assumed that all the wire segments have the same radius, conductivity and surface impedance.

In the DO LOOP ending with statement 20, SGANT calculates the segment lengths D(J). DMIN and DMAX denote the lengths of the shortest and longest segments. If the wire radius or the segment lengths are clearly beyond the range of thin-wire theory, N is set to zero at statement 25 followed by RETURN to the main program to abort the calculation.

At statement 30, the program selects a segment K, and a few statements below this it selects another segment L. K is a segment of test dipole I, and L is a segment of expansion mode J. The mutual impedance between segments K and L is obtained by calling subroutine GGS or GGM.



```

0001      2,*AM,BM,C,GD,CMM,D,EP2,EP3,ETA,FH2,GAM,SGD,X,Y,Z,LD,ZS)
0002      COMPLEX Z6,ZH,ZS,EGD,EGD,EGD,SGDS,SGDT,B01
0003      COMPLEX P11,P12,P21,P22,Q11,Q12,Q21,Q22,EP2,EP,ETA,GAM,EP3
0004      COMPLEX EPSILA,CHEA,BETA,ZARG
0005      COMPLEX P12,Z2,Q12,Z2,CGD(I),SGD(I),C(I),ZLD(I)
0006      DIMENSION X(1),Y(1),Z(1),D(1),IA(1),IB(1),MD(1),NM(4)
0007      DIMENSION I1(1),I2(1),I3(1),JA(1),JB(1),ND(1),ISC(1)
0008      DATA EO,TP,UO/8.54E-12,6.28318,1.2566E-6/
0009      FUIMAT(3X,'AM =',E10.3,3X,'DMAX =',E10.3,3X,'DMIN =',E10.3)
0010      EP=EP3
0011      ICC=(N#N+N)/2
0012      DO 10 I=1,ICC
0013      C(I)=(,0.,0)
0014      ZS(,0.,0)
0015      IF (CMM,LE,0.)GO TO 12
0016      OMEGA=TP*FH2
0017      EPSILA=CMPLX(EO,-CMM*1,E6/OMEGA)
0018      CHEA=(,0.1,)*OMEGA*EPSILA
0019      BETA=OMEGA*SQRT(UO)*CSQRT(EP)
0020      ZARG=BETA#AM
0021      CALL CBES(ZARG,B01)
0022      ZS=BE TA*B01/CHEA
0023      ZH=ZS/(TP*AM*GAM)
0024      DM IN=1,E30
0025      DMAX=,0
0026      DO 20 J=1,NM
0027      K=IA(J)
0028      L=IB(J)
0029      D(J)=SQRT((X(K)-X(L))**2+(Y(K)-Y(L))**2+(Z(K)-Z(L))**2)
0030      IF (D(J),LT,DMIN)DM IN=D(J)
0031      IF (D(J),GT,DMAX)DMAX=D(J)
0032      EGD=CEXP(GAM*DM IN)
0033      CGD(J)=(EGD+1,)/EGD)/2.
0034      SGO(J)=(EGD-1,)/EGD)/2.
0035      IF (DM IN,LT,2.*#AN)GO TO 25
0036      IF (CABS(GAM*AM),GT,0.06)GO TO 25
0037      IF (CABS(GAM*DMAX),GT,3.,)GO TO 25
0038      IF (AM,GT,0.)GO TO 30
0039      N=D
0040      WRITE(6,2)AM,DMAX,DM IN
0041      RETURN
0042      DO 200 K=1,NM
0043      NDK=ND(K)
0044      KA=IA(K)
0045      KB=IB(K)
0046      DK=D(K)
0047      CGDS=CGD(K)
0048      SGO S=SGD(K)
0049      DO 200 L=1,NM
0050      NDL=ND(L)
0051      LA=IA(L)
0052      LB=IB(L)
0053      DL=D(L)
0054      SGO T=SGD(L)
0055      NIL=0
0056      DO 200 I=1,NDK
0057      I=ND(K,II)
0058      MM=(I-1)#N-(I*1-1)/2
0059      FI=1.
0060      IF (KB,EQ,12(I))GO TO 36
0061      IF (KB,EQ,11(I))FI=-1.
0062

```

Fig. 8a. Subroutine SGANT

```

      15=1
      GO TO 40
36  IF (KA.EQ.13(1))FI=-1.
      IS=2
40  DO 200 JU=1,NDL
      MM=MM+J
      J=MD(L,J)
      IF (1.GT.J)GO TO 200
      FJ=1.
      IF (LB.EQ.12(J))GO TO 46
      IF (LB.EQ.11(J))FI=-1.
      JS=1
      GO TO 50
46  IF (LA.EQ.13(J))FJ=-1.
      JS=2
50  IF (NIL.NE.0)GO TO 168
      NIL=1
      IF (K.EQ.L)GO TO 120
      IND=(LA-KA)*(LB-KA)*(LA-KB)*(LB-KB)
      IF (IND.EQ.0)GO TO 80
      SEGMENTS K AND L SHARE NO POINTS
      CALL GGSIX(KA),Y(KA),Z(KA),X(KB),Z(KB),X(LA),Y(LA),Z(LA)
      3,P(1,1),P(1,2),P(2,1),P(2,2))
      GO TO 168
      SEGMENTS K AND L SHARE ONE POINT (THEY INTERSECT)
      KG=0
      JM=KB
      JC=KA
      JC=1
      IND=(KB-LA)*(KB-LB)
      IF (IND.NE.0)GO TO 82
      JC=KB
      KF=-1
      JM=KA
      KG=3
      LG=3
      JP=LA
      LE=-1
      IF (LB.EQ.JC)GO TO 83
      JP=LB
      LF=1
      LG=0
83  SGN=KF*LE
      CPSI=(X(JP)-X(JC))*(X(JM)-X(JC))*(Y(JP)-Y(JC))*(Y(JM)-Y(JC))
      2+Z(JP)-Z(JC))*(Z(JM)-Z(JC))/(DK*DL)
      CALL GGMH(.0,DK,.0,DL,AM,CGDS,SGDS,SGDT,CPSI,ETA,GAM
      2,0(1,1),0(1,2),0(2,1),0(2,2))
      DO 98 KK=1,2
      KP=IABS(KK-KG)
      DU 98 LL=1,2
      LP=IABS(LL-LG)
      P(KP,LP)=SGN*Q(KK,LL)
98  CONTINUE
      GO TO 168
      K=L (SELF REACTION OF SEGMENT K)
120  Q11=(0.,0)
      Q12=(0.,0)
      IF (CMM.LE.0.)GO TO 150
      GD=GAM*DK
      ZG=ZL/(SGDS**2)
      Q11=ZG*(SGDS*CGDS-GD)/2.

```

Fig. 8b. Subroutine SGANT

22

```

0063'
0064
0065
0066
0067
0068
0069
0070
0071
0072
0073
0074
0075
0076
0077
0078
0079
0080
0081
0082
0083
0084
0085
0086
0087
0088
0089
0090
0091
0092
0093
0094
0095
0096
0097
0098
0099
0100
0101
0102
0103
0104
0105
0106
0107
0108
0109
0110
0111
0112
0113
0114
0115
0116
0117
0118
0119
0120
0121
0122
0123
0124

      Q12=ZG*(GD*CGDS-SGDS)/2.
150  ISCK=ISCK(I)
      P11=(0.,0)
      P12=(0.,0)
      IF (ISCK.EQ.0)GO TO 155
      IF (BM.LE.AM)GO TO 155
      CALL
      DSHELL(AM,BM,DK,CGDS,SGDS,EP2,EP,ETA,GAM,P11,P12)
155  Q11=P11+Q11
      Q12=P12+Q12
      CALL GGMH(.0,DK,.0,DL,AM,CGDS,SGDS,SGDT,CPSI,ETA,GAM,P11,P12)
      2,ETA,GAM,P11,P12,P21,P22)
      Q11=P11+Q11
      Q12=P12+Q12
      P(1,1)=Q11
      P(1,2)=Q12
      P(2,1)=Q12
      P(2,2)=Q11
      IF (KA.NE.LA)GO TO 160
      GO TO 168
160  P(1,1)=-Q12
      P(1,2)=-Q11
      P(2,1)=-Q11
      P(2,2)=-Q12
168  C(MMH)=C(MMH)+F1*FJ*JP(15,JS)
200  CONTINUE
      DO 220 I=1,N
      IJ=(I-1)*N-(I*I-1)/2+1
      J1=JA(I)
      IF (I2(I).EQ.1B(J1))J1=J1+NM
      J2=JB(I)
      IF (I2(I).EQ.1B(J2))J2=J2+NM
      C(I,J)=C(I,J)+ZLD(J1)+ZLD(J2)
220  RETURN
      END

```

Fig. 8c. Subroutine SGANT

23

In statement 168, this impedance is lumped into  $C(MMM)$ . The mutual impedance  $Z_{ij}$  between dipoles I and J is the sum of four segment-segment impedances.

In SGANT, segment K has endpoints KA and KB, and segment L has endpoints LA and LB. It is convenient to think of KA and KB as points 1 and 2 on segment K, and LA and LB as points 1 and 2 on L. Now we define four segment-segment impedances  $P(IS,JS)$ . The first subscript IS refers to the terminal point on segment K, and the second subscript JS refers to the terminal point on L. Thus  $IS = 1$  or  $2$  if dipole I has its terminal point I2(1) at KA (point 1) or KB (point 2), respectively. Similarly,  $JS = 1$  or  $2$  if mode J has its terminal point I2(J) at LA or LB. The impedances  $P(IS,JS)$  are defined with the following reference directions for current flow: from point 1 toward point 2 on each segment. If dipole I has this same reference direction on segment K, we set  $FI = 1$ ; otherwise  $FI = -1$ . Similarly  $FJ = 1$  or  $-1$  in accordance with the reference direction for mode J on segment L. In statement 168,  $P(IS,JS)$  is multiplied by  $FI$  and  $FJ$  before its contribution is added to  $Z_{ij}$ .

Subroutine GGM calculates the impedances  $Q(KK,LL)$  which are like the  $P(IS,JS)$  but have different conventions for reference directions and subscript meaning. The transformation from the  $Q$  impedances to the  $P$  impedances is accomplished in the DO LOOP ending with statement 98.

If the wire has finite conductivity, the appropriate modification is applied to the impedance matrix just above statement 150. (See Eqs. 27 through 29 in Reference 1.) The terms arising from the dielectric shell on an insulated segment are obtained from subroutine DSHLL just above statement 155. Finally, the lumped loads  $ZLD$  are added to the diagonal elements of the impedance matrix in statement 220.

The impedance matrix could be calculated in a different order as follows. Select modes I and J, calculate  $ZIJ$ , and then increment I or J. Instead, SGANT selects segments K and L, calculates  $ZKL$ , adds  $ZKL$  to all the appropriate elements  $ZIJ$ , and then increments K or L. This minimizes the calls to GGS and GGM and presumably improves the computational efficiency.

K is a segment of test dipole I, and L is a segment of expansion mode J. When the segment numbers K and L are equal, SGANT calls GGM to obtain the mutual impedance between two filamentary electric monopoles. These monopoles are parallel and have the same length. Monopole K is positioned on the axis of the wire segment, and monopole L is on the surface of the same wire segment. Thus, the displacement is equal to the wire radius. The two monopoles are side-by-side with no stagger.

When segments K and L intersect, SGANT again calls GGM for the mutual impedance between the two filamentary monopoles. Monopole K is

situated on the axis of wire segment K, and monopole L is on the surface of wire segment L. The axes of segments K and L define a plane P, and monopole K lies in this plane. Monopole L is parallel with plane P and is displaced from it by a distance equal to the wire radius.

#### APPENDIX 3. Subroutine CBES

Subroutine CBES, listed in Fig. 9, calculates the quantity  $B01 = J_0(z)/J_1(z)$  where  $z$  is complex and  $J_0$  and  $J_1$  denote the Bessel functions of order zero and one.

#### APPENDIX 4. Subroutine DSHLL

Subroutine DSHLL, listed in Fig. 10, calculates the mutual impedance term contributed by the dielectric insulation on the surface of a thin wire. This subroutine uses Eq. 35 of Reference 1.

#### APPENDIX 5. Subroutine GGS

Subroutine GGS, listed in Fig. 11, calculates the mutual impedance between two filamentary monopoles with sinusoidal current distributions. (The dipole-dipole mutual impedance in Eq. 20 of Reference 1 is the sum of four monopole-monopole mutual impedances.) The endpoints of the axial test monopole s are  $(XA,YA,ZA)$  and  $(XB,YB,ZB)$ , and the endpoints of the expansion monopole t are  $(X1,Y1,Z1)$  and  $(X2,Y2,Z2)$ . DS and DT denote the lengths of monopoles s and t, respectively. CAS, CBS and GGS are the direction cosines of monopole s, and CA, CB and CG are the direction cosines of monopole t.

If  $INT = 0$ , GGS calls GGM for the closed-form impedance calculations. Otherwise GGS calculates the mutual impedance via Simpson's-rule integration with the following number of sample points:  $IP = INT + 1$ . If the monopoles are parallel with small displacement, GGS calls GGM to avoid the difficulties of numerical integration.

For the fields of the test monopole, GGS uses Eqs. 75 and 76 of Reference 1. The current distribution on the expansion monopole is given by Eq. 74 of Reference 1. With an origin at  $(X1,Y1,Z1)$ , the coordinate T measures distance along the expansion monopole. Thus T is the integration variable.

Let the coordinate s measure distance along the test monopole with origin at  $(XA,YA,ZA)$ . From any point T on monopole t, construct a line to the test monopole such that the line is perpendicular to the test monopole. SZ denotes the s coordinate of the intersection of this line with the test monopole. The length of the line is the radial coordinate  $\rho$ , and RS denotes  $\rho^2$ . R1 and R2 are the distances from  $(XA,YA,ZA)$  and  $(XB,YB,ZB)$  to the point T. C1 is the current at T for the mode with terminals at  $(X1,Y1,Z1)$ , and C2 is the current at T for the other mode with terminals at  $(X2,Y2,Z2)$ . C denotes the Simpson's-rule weighting coefficient.



```

SUBROUTINE CBES(Z,B01)
  COMPLEX ARG,CC,CS,EX
  COMPLEX B01,Z,TERMJ,TERMN,MZ24,N(2)
  DATA PI/3.14159/
  IF (CABS(Z).GE.12.0) GO TO 10
  FACTOR=0.0
  TERMN=(0.,0.)
  MZ24=-0.25*Z
  TERMJ=(1.0,0.0)
  DO 1 NP=1,2
    N=NP-1
    UN(INP)=TERMJ
    M=0
    2 M=M+1
    TERMJ=TERMJ*MZ24/FACT(M*(N+M))
    UN(NP)=UN(NP)+TERMJ
    IF (NP.NE.1) GO TO 3
    FACTOR=FACTOR+1.0/FACT(M)
    TERMN=TERMN+TERMJ*FACTOR
    3 EROR=CABS(TERMJ)
    IF (EROR.GT.1.0E-10) GO TO 2
    1 TERMJ=0.5*Z
    B01=UN(1)/UN(2)
    RETURN
  10 Y=AIMAG(Z)
    IF (ABS(Y).GT.20.)GO TO 20
    ARG=(0.,1.)*Z
    EX=CEXP(ARG)
    CC=EX+1./EX
    CS=(1.0,-1.)*(EX-1./EX)
    B01=(CS+CC)/(CS-CC)
    RETURN
  20 B01=(1.0,-1.)
    IF (V.LT.0.)B01=(1.0,1.)
    RETURN
  END

```

Fig. 9. Subroutine CBES

```

0001
0002
0003
0004
0005
0006
0007
0008
0009
0010
0011
0012
0013
0014
0015
0016
0017
0018
0019
0020
0021
0022
0023
0024
0025
0026
0027
0028
0029
0030
0031
0032
0033
0034
0035
0036

```

```

SUBROUTINE DSHELL(AM,BM,DK,SGDS,EP2,EP,ETA,GAM,P11,P12)
  COMPLEX CGDS,SGDS,EP2,EP,ETA,GAM,P11,P12,GD,CST
  DATA PI/3.14159/
  GD=GAM*DK
  CST=(EP2-EP)*ETA*ALOG(BM/AM)/(4.*PI*EP2*SGDS*SGDS)
  P11=-CST*(GD+SGDS*CGDS)
  P12=CST*(GD*CGDS+SGDS)
  RETURN
  END

```

```

0001
0002
0003
0004
0005
0006
0007
0008
0009

```

Fig. 10. Subroutine DSHELL.

```

SUBROUTINE GGS(XA,YA,ZA,XB,YB,ZB,X1,Y1,Z1,X2,Y2,Z2,AM
2DGS,CGDS,SGDS,DT,SGDT,INT,ETAGAM,P11,P12,P21,P22)
COMPLEX P11,P12,P21,P22,EJA,EJB,EJ1,EJ2,ETAGAM,C1,C2,CST
DATA P/12.56637/
CA=(X2-X1)/DT
CB=(Y2-Y1)/DT
CG=(Z2-Z1)/DT
CAS=(XB-XA)/DS
CBS=(YB-YA)/DS
CGS=(ZB-ZA)/DS
CC=CA*CB+CB*CGS+CG*CGS
IF(IABS(CC).GT..997)GO TO 200
SZ=(X1-XA)*CAS+(Y1-YA)*CBS+(Z1-ZA)*CGS
IF(INT-LE..0)GO TO 300
INS=2*(INT/2)
IF(INS.LT..2)INS=2
IP=INS+1
DELT=DT/INS
T=.0
DSZ=CC*DELT
P11=(.0,.0)
P12=(.0,.0)
P21=(.0,.0)
P22=(.0,.0)
1000 AMS=AM*AM
5000 SGN=-1.
EJDO=100 IN=1,IP
+0.50 Z1=SZ
+0.50 Z2=SZ-DS
+0.00 XZ=X1+T*CA-XA-SZ*CAS
+0.00 YZ=Y1+T*CB-YA-SZ*CBS
+0.00 ZZ=Z1+T*CG-ZA-SZ*CGS
E000RS=XZ+2*YZ+2*ZZ*2
R1=SQRT(RS+Z1*2)
EJA=CEXP(-GAM*R1)
EJB=CEXP(-GAM*R1)
R2=SQRT(RS+Z2*2)
EJ2=CEXP(-GAM*R2)
EJ1=EJA/R1
EJ2=EJB/R2
ER1=EJA*SGDS+Z1*WEJ1*CGDS-Z2*WEJ2
ER2=EJB*SGDS+Z2*WEJ2*CGDS-Z1*WEJ1
FAC=.0
IF(RS.GT.AMS)FAC=(CA*XXZ+CB*YZ+CG*ZZ)/RS
ET1=CC*(EJ2-EJ1*CGDS)+FAC*ER1
ET2=CC*(EJ1-EJ2*CGDS)+FAC*ER2
C=3.+SGN
IF(IN.EQ.1..OR..IN.EQ.IP)C=1.
EGD=CEXP(GAM*(DT-T))
C1=C*(EGD-1.)/(EGD)/2.
EGD=CEXP(GAM*T)
C2=C*(EGD-1.)/(EGD)/2.
P11=P11+ET1*C1
P12=P12+ET1*C2
P21=P21+ET2*C1
P22=P22+ET2*C2
T=T+DELT
SZ=SZ+DSZ
SGN=-SGN
100 CST=-ETAGAM/DT/(3.*F*P*SGDS*SGDT)
P11=CST*P11
P12=CST*P12

```

Fig. 11a. Subroutine GGS

28

```

P21=CST*P21
P22=CST*P22
RETURN
200
SZ1=(X1-XA)*CAS+(Y1-YA)*CBS+(Z1-ZA)*CGS
RH1=SQRT((X1-XA-SZ1*CAS)**2+(Y1-YA-SZ1*CBS)**2+(Z1-ZA-SZ1*CGS)**2)
SZ2=SZ1+T*CC
RH2=SQRT((X2-XA-SZ2*CAS)**2+(Y2-YA-SZ2*CBS)**2+(Z2-ZA-SZ2*CGS)**2)
DDO=(RH1+RH2)/2.
IF(DDO.GT..20.*AM..AND..INT.GT..0)GO TO 20
IF(DDO.LT..AM)DDO=AM
CALL GGMH(.0,DS,SZ1,SZ2,DDO,CGDS,SGDS,SGDT,1.
2.ETAGAM,P11,P12,P21,P22)
RETURN
300
SS=SQRT(1.-CC*CC)
CAD=(CGS*CB-CBS*CG)/SS
CBD=(CAS*CG-CGS*CA)/SS
CGD=(CBS*CA-CAS*CB)/SS
DK=(X1-XA)*CAD+(Y1-YA)*CBD+(Z1-ZA)*CGD
DK=ABS(DK)
IF(DK.LT..AM)DK=AM
XZ=XA+SZ*CAS
YZ=YA+SZ*CBS
ZZ=ZA+SZ*CGS
XP1=X1-DK*CAD
YP1=Y1-DK*CBD
ZP1=Z1-DK*CGD
CAP=CBS*CGD-CGS*CGD
CBP=CGS*CAD-CAS*CGD
CP1=CAP*(XP1-XZ)+CBP*(YP1-YZ)+CGP*(ZP1-ZZ)
T1=PI/SS
SI=TI*CC-SZ
CALL GGMH(SI,S1+DS,T1,T1+DT,DK,CGDS,SGDS,SGDT,CC,ETAGAM
2,P11,P12,P21,P22)
RETURN

```

Fig. 11b. Subroutine GGS

29

Below statement 300, GGS performs some analytic geometry in preparation for calling GGM. The remaining part of this Appendix concerns this last part of subroutine GGS.

Let  $\hat{s}$  denote a unit vector in the direction from  $(X_A, Y_A, Z_A)$  toward  $(X_B, Y_B, Z_B)$ . Also let  $\hat{t}$  denote a unit vector from  $(X_1, Y_1, Z_1)$  toward  $(X_2, Y_2, Z_2)$ . Then  $\hat{s} \cdot \hat{t} = \cos \theta = CC$  where  $\theta$  is the angle formed by the axes of the two monopoles. Let monopole  $s$  lie in one plane  $P_s$  and monopole  $t$  lie in another parallel plane  $P_t$ .  $CAD$ ,  $CBP$  and  $CGP$  are the direction cosines of the unit vector  $\hat{d} = \hat{t} \times \hat{s} / \sin \theta$  which is perpendicular to both planes. To obtain the distance  $DK$  between the two planes, we construct a vector  $R_{11}$  from  $(X_A, Y_A, Z_A)$  to  $(X_1, Y_1, Z_1)$  and take  $DK = R_{11} \cdot \hat{d}$ .

Construct a line from  $(X_1, Y_1, Z_1)$  to the test monopole, such that the line is perpendicular to the test monopole.  $SZ$  denotes the  $s$  coordinate of the intersection of this line with the test monopole, and the cartesian coordinates of this intersection are  $XZ$ ,  $YZ$  and  $ZZ$ . The direction cosines of  $\hat{s} \times \hat{d}$  are  $CAP$ ,  $CBP$  and  $CGP$ .

From the point  $(X_1, Y_1, Z_1)$  in plane  $P_t$ , construct a perpendicular line to the point  $(X_P, Y_P, Z_P)$  in the plane  $P_s$ . This line is parallel with  $\hat{d}$  and has length  $DK$ . Let  $R$  represent a vector from  $(XZ, YZ, ZZ)$  to  $(X_P, Y_P, Z_P)$ .  $P1$  denotes  $R \cdot (\hat{s} \times \hat{d})$ .  $S1$  and  $T1$  are defined in the next Appendix.

#### APPENDIX 6. Subroutine GGM

Subroutine GGM calculates the mutual impedance between two filamentary monopoles with sinusoidal current distributions. The dipole-monopole mutual impedance in Eq. 20 of Reference 1 is the sum of four monopole-monopole mutual impedances. The monopole impedances are calculated by GGS with Simpson's rule or by GGM with closed-form expressions in terms of exponential integrals.

To explain the input data for GGM, reference is made to Fig. 12. Subroutine GGM is listed in Fig. 13. If the monopoles are parallel, let the  $z$  axis be parallel with both monopoles. The coordinate origin may be selected arbitrarily.  $S1$  and  $S2$  denote the  $z$  coordinates of the endpoints of the test monopole,  $T1$  and  $T2$  are the  $z$  coordinates of the endpoints of the expansion monopole, and  $D$  is the perpendicular distance (displacement) between the monopoles. The mutual impedance of parallel monopoles is calculated in the last part of GGM below statement 110.

For skew monopoles, let the test monopole  $s$  lie in the  $xy$  plane and the expansion monopole  $t$  in the plane  $z = D$ . ( $D$  is the perpendicular distance between the parallel planes.) If the monopoles are viewed along a line of sight parallel with the  $z$  axis as in Fig. 12, the extended axes of the two monopoles will appear to intersect at a point on the  $xy$  plane. Let  $s$  measure the distance along the axis of

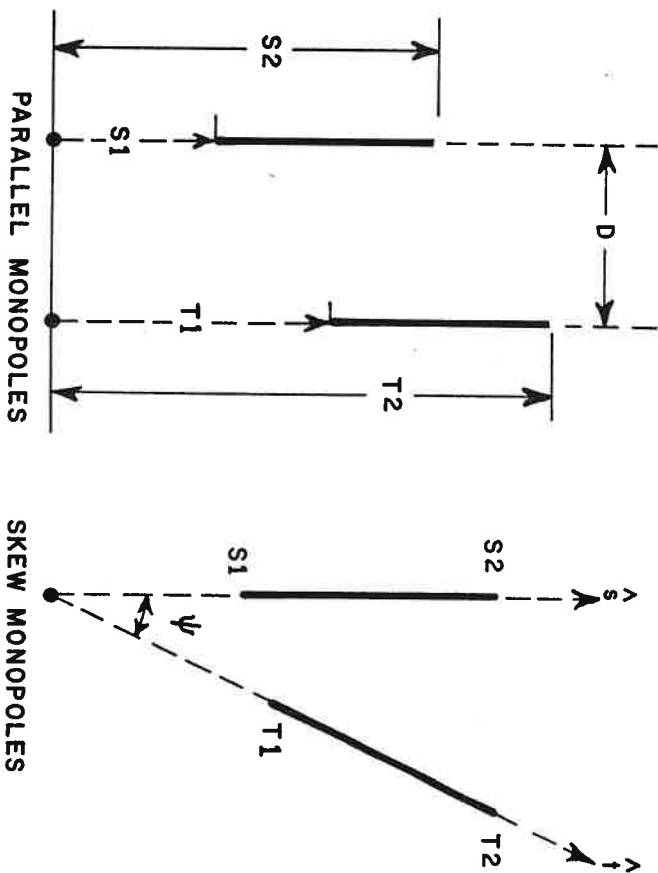


Fig. 12. Coordinates for parallel and skew monopoles in subroutine GGM.



```

SUBROUTINE GGMW(S1,S2,T1,T2,D,CGD5,SGD1,SGD2,CPS1,ETA,GAM
2,P11,P12,P21,P22)
DOUBLE PRECISION R1,R2,DPO,SIS,TIS,ST2,ST1,ST2,CD,BD,CPS5,SK
2,T11,T12,TD1,TD2,SD1,DPS1,BD,ZD
COMPLEX CGD5,SGD5,SGD1,SGD2,ETA,GAM,P11,P12,P21,P22
COMPLEX CST,EB,EC,EK,ELE,EKL,EGZ1,ES1,ES2,ET1,ET2,EXPB,EXPB
COMPLEX EGZ1(2),F(2,2),GM(2),GP(2)
DATA PI/3.14159/
DSQ=D*0
SGD5=SGD1
IF (S2.LT.S1) SGD5=-SGD1
SGD1=SGD2
IF (T2.LT.T1) SGD1=-SGD2
IF (ABS(CPS1).GT.0.997) GO TO 110
ES1=CEXP(GAM*S1)
ES2=CEXP(GAM*S2)
E11=CEXP(GAM*T1)
E12=CEXP(GAM*T2)
DO=D
DPS1=CPS1
T01=T1
T02=T2
CPS5=DPS1*0.0PS1
CD=UD/D*SQRT(1.0D-CPS5)
C=CD
BD=CD*0.0PS1
B=BD
EB=CEXP(GAM*CMPLX(0.0,B))
EC=CEXP(GAM*CMPLX(0.0,C))
DO 10 K=1,2
E(K,L)=(0.0,0)
T1=TD1*TD1
T2=TD2*TD2
DPO=DD*DD
S1=S1
DO 100 I=1,2
FI=(-1)**I
SD1=SI
SIS=SD1*SD1
ST1=2.*SD1*TD1*0.0PS1
ST2=2.*SD1*TD2*0.0PS1
R1=DSQRT(DPO+SIS+TIS-ST1)
R2=DSQRT(DPO+SIS+TIS-ST2)
EK=EB
DO 50 K=1,2
FK=(-1)**K
SK=FK*SD1
EL=EC
DO 40 L=1,2
FL=(-1)**L
XK=FK*BD+FL*CD
XL=EK*EL
TL1=FL*TD1
TL2=FL*TD2
R1=R1*SK+TL1
R2=R2*SK+TL2
CALL EXPJ(GAM*CMPLX(RR1,-XX),GAM*CMPLX(RR2,-XX),EXPB)
CALL EXPJ(GAM*CMPLX(RR1,XX),GAM*CMPLX(RR2,XX),EXPB)
E(K,L)=E(K,L)+I*(EXPB*EK+EXPB/EKL)
EL=1./EC

```

Fig. 13a. Subroutine GGMW

32

```

0001 0001
0002 0002
0003 0003
0004 0004
0005 0005
0006 0006
0007 0007
0008 0008
0009 0009
0010 0010
0011 0011
0012 0012
0013 0013
0014 0014
0015 0015
0016 0016
0017 0017
0018 0018
0019 0019
0020 0020
0021 0021
0022 0022
0023 0023
0024 0024
0025 0025
0026 0026
0027 0027
0028 0028
0029 0029
0030 0030
0031 0031
0032 0032
0033 0033
0034 0034
0035 0035
0036 0036
0037 0037
0038 0038
0039 0039
0040 0040
0041 0041
0042 0042
0043 0043
0044 0044
0045 0045
0046 0046
0047 0047
0048 0048
0049 0049
0050 0050
0051 0051
0052 0052
0053 0053
0054 0054
0055 0055
0056 0056
0057 0057
0058 0058
0059 0059
0060 0060
0061 0061
0062 0062

50 EK=1./EB
ZD=SD1*0.0PS1
ZC=ZD
EGZ1=CEXP(GAM*ZC)
R1=R1+ZD-TD1
R2=R2+ZD-TD2
CALL EXPJ(GAM*RR1,GAM*RR2,EXPB)
F(1,1)=2.*SGD5*EXPB/EGZ1
F(1,2)=2.*SGD5*EXPB/EGZ1
S1=S2
CST=ETA/(16.*PI*SGD5*SGD1)
P11=CST*(F(1,1)+E(2,2)*ES2-E(1,2)/ES2)*ET2
A +(-F(1,2)-E(2,1)*ES2+E(1,2)/ES2)/ET2
P12=CST*(F(1,1)-E(2,2)*ES2+E(1,2)/ES2)*ET1
B +(-F(1,2)+E(2,1)*ES2-E(1,2)/ES2)/ET1
P21=CST*(F(2,1)-E(2,2)*ES1+E(1,2)/ES1)*ET2
C +(-F(2,2)+E(2,1)*ES1-E(1,2)/ES1)/ET2
P22=CST*(F(2,1)+E(2,2)*ES1-E(1,2)/ES1)*ET1
D +(-F(2,2)-E(2,1)*ES1+E(1,2)/ES1)/ET1
RETURN
110 IF(CPS1.LT.0.) GO TO 120
IA=TI
TB=T2
GO TO 130
120 TA=TI
TB=T2
SGD1=-SGD1
130 SI=S1
DO 150 I=1,2
TJ=TA
ZIU=TJ-SI
R=SQRT(DSQ+ZIU*ZIU)
W=R+ZIU
IF(ZIU.LT.0.) W=-DSQ/(R-ZIU)
V=R-ZIU
IF(ZIU.GT.0.) V=DSQ/(R+ZIU)
IF(J.EQ.1) V1=V
IF(J.EQ.1) W1=W
EGZ1(J)=CEXP(GAM*ZIU)
140 TJ=TB
CALL EXPJ(GAM*W1,GAM*W,GP(1))
CALL EXPJ(GAM*W1,GAM*W,GP(1))
S1=S2
CST=-ETA/(8.*PI*SGD5*SGD1)
P11=CST*(GM(2)*EGZ1(2)+GP(2)/EGZ1(2)+2)
2-CGD5*(GM(1)*EGZ1(1,2)+GP(1)/EGZ1(1,2))
P12=CST*(GM(2)*EGZ1(2,1)-GP(2)/EGZ1(2,1))
2+CGD5*(GM(1)*EGZ1(1,1)+GP(1)/EGZ1(1,1))
P21=CST*(GM(1)*EGZ1(1,2)+GP(1)/EGZ1(1,2))
2-CGD5*(GM(2)*EGZ1(2,2)+GP(2)/EGZ1(2,2))
P22=CST*(GM(1)*EGZ1(1,1)-GP(1)/EGZ1(1,1))
2+CGD5*(GM(2)*EGZ1(2,1)+GP(2)/EGZ1(2,1))
RETURN
END

```

Fig. 13b. Subroutine GGMW

33

the test monopole with origin at the apparent intersection. S1 and S2 denote the s coordinates of the endpoints of the test monopole. Similarly, let t measure distance along the axis of the expansion monopole with origin at the apparent intersection. T1 and T2 denote the t coordinates of the endpoints of the expansion monopole. Let  $\hat{s}$  and  $\hat{t}$  be unit vectors parallel with the positive s and t axes, respectively. Then  $\text{CPSI} = \hat{s} \cdot \hat{t} = \cos \psi$ . The monopole lengths are  $d_s$  and  $d_t$ , and the remaining input data are defined as follows:

```
CGDS      cosh yds
SGD1      sinh yds
SGD2      sinh ydt
```

GGMM calls EXPJ for the exponential integrals.

The output data from GGMM are the impedances P11, P12, P21, and P22. In defining these impedances, the reference direction is from S1 to S2 for the current on monopole s, and from T1 to T2 for the current on monopole t. In the impedance P1j, the first subscript is 1 or 2 if the test dipole has terminals at S1 or S2 on monopole s. The second subscript is 1 or 2 if the expansion dipole has terminals at T1 or T2 on monopole t. The endpoint coordinates S1, S2, T1 and T2 may be positive or negative. The monopole lengths  $d_s$  and  $d_t$  are assumed positive in defining the input data CGDS, SGD1 and SGD2.

For parallel monopoles,  $\text{CPSI} = 1$  or  $-1$ . S1, S2, T1 and T2 are cartesian coordinates for parallel monopoles and spherical coordinates for skew monopoles. For skew monopoles, the radial coordinates S1, S2, T1 and T2 tend to infinity as the angle  $\psi$  tends to zero or  $\pi$ . Therefore, if the monopoles are within  $4.5^\circ$  of being parallel, they are approximated by parallel dipoles.

#### APPENDIX 7. Subroutine EXPJ

Subroutine EXPJ, listed in Fig. 14, evaluates the exponential integral defined as follows:

$$(2) \quad W12 = \int_{V1}^{V2} \frac{e^{-V}}{V} dV = E_1(V1) - E_1(V2) + j 2\pi$$

where the integration path is the straight line from V1 to V2 on the complex v plane and

$$(3) \quad E_1(z) = \int_z^\infty \frac{e^{-t}}{t} dt$$

```

SUBROUTINE EXPJ(V1,V2,N12)
  COMPLEX EC,E15,S,T,UC,VC,V1,V2,W12,Z
  DIMENSION V(12),M(12),D(16),E(16)
  DATA V/ 0.22284667E 00,
20.11889321E 01,0.29927363E 01,0.57751436E 01,0.98376674E 01,
20.15982874E 02,0.93307812E 01,0.49289174E 00,0.12155954E 01,
20.22699495E 01,0.36676227E 01,0.54253366E 01,0.75659162E 01,
20.10120222E 02,0.13130282E 02,0.16654408E 02,0.20776479E 02,
20.25623894E 02,0.31407519E 02,0.38530683E 02,0.48026086E 02/
  DATA M/ 0.5896460E 00,
20.41700083E 00,0.11337338E 00,0.10399197E 01,0.26101720E 03,
20.89854791E 06,0.21823487E 00,0.34221017E 00,0.26302738E 00,
20.12642582E 00,0.40206865E 01,0.85638778E 02,0.12124361E 02,
20.1167440E 03,0.64599267E 05,0.16654169E 06,0.42274304E 08,
20.39218973E 10,0.14565152E 12,0.14830270E 15,0.16005949E 19/
  DATA D/ 0.22495842E 02,
2 0.74411568E 02,-0.41431576E 03,-0.78754339E 02,0.11254744E 02,
2 0.16021761E 03,-0.23862195E 03,-0.50094487E 03,-0.68487854E 02,
2 0.12254778E 02,-0.10161976E 02,-0.47719591E 01,0.79729681E 01,
2 0.21069574E 02,0.22046490E 01,0.89728244E 01/
  DATA E/ 0.21103107E 02,
2 0.37959787E 03,-0.97489220E 02,0.12900672E 03,0.17949226E 02,
2 0.12910931E 03,-0.55705574E 03,0.13524801E 02,0.14696721E 03,
2 0.17949528E 02,-0.32981014E 00,0.31028836E 02,0.81657657E 01,
2 0.22236661E 02,0.39124892E 02,0.81636799E 01/
  Z=V1
  DO 100 JIM=1,2
    X=REAL(Z)
    Y=AIMAG(Z)
    E15=(0.0,0)
    AB=CABS(Z)
    IF (AB.EQ.0.0) GO TO 90
    IF (X.GE.0.0) .AND. AB.GT.10.0 GO TO 80
    IF (X.LE.0.0) .AND. YA.GT.10.0 GO TO 80
    IF (YA-X.GE.17.5) OR YA.GE.6.5) OR X*YA.GE.5.5) OR X.GE.3.0) GO TO 20
    IF (X.LE.-9.0) GO TO 40
    IF (X-X.GE.-2.5) GO TO 50
    IF (Y+YA.GE.1.5) GO TO 30
    N=6+3*AB
    E15=1.0/(N-1.0)-Z/N**2
    N=N-1
    E15=1.0/(N-1.0)-Z*E15/N
    IF (N.GE.-3) GO TO 15
    E15=Z*E15-CMPLX(.5772156+ALD6(AB),ATM2(Y,X))
    GO TO 90
  10 J1=1
  15 J2=6
  20 J1=1
  20 J2=6
  30 J1=7
  30 J2=21
  31 S=(0.0,0)
  YS=Y*Y
  DO 32 I=J1,J2
    X1=V(11)+X
    CF=M(11)/(X1*X1+YS)
    S=S+CMPLX(X1*CF,-YA*CF)
  32 GO TO 54
  40 T3=X*X-Y*Y
  40 T4=2.*X*YA
  40 T5=X*T3-YA*T4
  40 T6=X*T4+YA*T3

```

Fig. 14a. Subroutine EXPJ

```

      UC=CMPLX(D(11)+D(12)*X+D(13)*T3+D(14)*T5-E(12)*YA-E(13)*T4,
0063      E(11)+E(12)*X+E(13)*T3+D(12)*YA+D(13)*T4,
0064      VC=CMPLX(D(14)+D(15)*X+D(16)*T3+D(15)*YA-E(16)*T4,
0065      E(14)+E(15)*X+E(16)*T3+D(15)*YA+D(16)*T4,
0066      GO TO 52
0067      T3=X*X-Y*Y
0068      T4=2.*X*YA
0069      T5=X*T3-YA*T4
0070      T6=X*T4+YA*T3
0071      T7=X*T5-YA*T6
0072      T8=X*T6+YA*T5
0073      T9=X*T7-YA*T8
0074      T10=X*T8+YA*T7
0075      UC=CMPLX(D(11)+D(12)*X+D(13)*T3+D(14)*T5+D(15)*T7+D(16)*T9-E(12)*YA-E(13)*T4,
0076      2+E(14)*T6+E(15)*T8)+E(11)+E(12)*X+E(13)*T3+E(14)*T5+E(15)*T7+D(16)*T9+
0077      3(D(12)*YA+D(13)*T4+D(14)*T6+D(15)*T8))
0078      VC=CMPLX(D(14)+D(15)*X+D(16)*T3+D(15)*YA+D(16)*T4,
0079      2+E(16)*T6+E(17)*T8)+E(14)+E(15)*T3+E(16)*T5+E(17)*T7+D(18)*T9+
0080      3(D(17)*YA+D(18)*T4+D(19)*T6+D(10)*T8))
0081      EC=UC/VC
0082      S=EC/CMPLX(X,YA)
0083      EX=EXP(-X)
0084      E15=S*T
0085      T=EX*CMPLX(COS(YA),-SIN(YA))
0086      E15=S*T
0087      IF(YA.LT.0.)E15=CONJG(E15)
0088      GO TO 90
0089      E15=-.409319/(Z+.193044)+.421831/(Z+1.02666)+.147126/(Z+2.56788)+
0090      2.206335E-1/(Z+.90035)+.107401E-2/(Z+.18215)+.158654E-4/(Z+
0091      312.7342)+.317031E-7/(Z+.39577)
0092      E15=E15*CEXP(-Z)
0093      IF(UIM.EQ.1)M12=E15
0094      Z=VZ
0095      T=ATAN2(AIMAG(Z),REAL(Z))-ATAN2(AIMAG(V2),REAL(V2))
0096      2*ATAN2(AIMAG(V1),REAL(V1))
0097      AB=ABS(TH)
0098      IF(AB.LT.1.)TH=.0
0099      IF(TH.GT.1.)TH=.2831853
0100      IF(TH.LT.-1.)TH=-.2831853
0101      M12=M12-E15+CMPLX(.0,TH)
0102      RETURN
0103      END
0104

```

Fig. 14b. Subroutine EXPJ

The exponential integral  $E_1(z)$  is defined in Reference 3. To generate W12, subroutine EXPJ calculates  $E_1(V1)$ , subtracts  $E_1(V2)$  and adds  $j2\pi$ . The term  $j2\pi$  is determined by the requirement that W12 vanish in the limit as  $V1$  approaches  $V2$ . The integer  $n$  may assume values of -1, 0 or +1. If the integration path does not cross the negative real axis in the  $v$  plane,  $n$  is zero. The term  $j2\pi$  is calculated below statement 100C.

#### APPENDIX 8. Subroutine GANTI

Subroutine GANTI, listed in Fig. 15, considers the wire structure as an antenna. In the input data,  $Vg(j)$  is the voltage of a generator at point  $1A(j)$  of segment  $j$ .  $Vg(j)$  is the voltage of a generator at point  $1B(j)$  of segment  $j$ . The D0 LOOP ending with statement 50 uses the delta-gap model to determine the excitation voltages  $Cj(I)$  for all the dipole modes. These are also stored temporarily in  $Cg(I)$ . Then subroutine SQR0T is called to obtain a solution of the simultaneous linear equations. SQR0T stores the solution (the loop currents) in  $Cj(I)$ .

In the D0 LOOP ending at statement 80, the complex power input is calculated and stored in Y11.  $Gg$  denotes the time-average power input and is the real part of Y11. If the antenna has only one voltage generator (with unit voltage and zero phase angle), then Y11 also denotes the antenna admittance and Z11 is the antenna impedance at that port.

Subroutine RTE is called to make the transformation from the loop currents  $Cj(I)$  to the branch currents  $Cg(j)$ . If IWR is a positive integer, RTE will write out the list of branch currents.

Finally, GANTI calculates the radiation efficiency EFF. PIN denotes the time-average power input. Subroutine GDISS is called to obtain the time-average power dissipated. DISS is the total power dissipated in the lumped loads and the imperfectly-conducting wire. PRAD is the time-average power radiated, defined by the difference between PIN and DISS. If the antenna has perfect conductivity and purely reactive loads, the radiation efficiency is considered to be 100 per cent.

#### APPENDIX 9. Subroutine SQR0T

Subroutine SQR0T is listed in Fig. 16. This subroutine considers the matrix equation  $ZI = V$  which represents a system of simultaneous linear equations. If the square matrix  $Z$  is symmetric, SQR0T is useful for obtaining the solution  $I$  with  $V$  given. NEQ denotes the number of simultaneous equations and the size of the matrix  $Z$ .

On entry to SQR0T,  $S$  is the excitation column  $V$ . On exit, the solution  $I$  is stored in  $S$ . Let  $Z(i,j)$  denote the symmetric square



```

SUBROUTINE GANTI(IA,IB,INM,IMR,I1,I2,I3,I12,I13,JA,JB,MD,N,ND,NM,AM
2,C,CJ,CG,CMH,DD,EFF,GAM,GG,CGD,SGD,VG,YI1,ZI1,ZLD,ZS)
0001
0002
0003
0004
0005
0006
0007
0008
0009
0010
0011
0012
0013
0014
0015
0016
0017
0018
0019
0020
0021
0022
0023
0024
0025
0026
0027
0028
0029
0030
0031
0032
0033
0034
0035
0036
0037
0038
0039
0040
DIMENSION D(1),IA(1),IB(1),IMR(1),JA(1),JB(1)
DIMENSION I1(1),I2(1),I3(1),MD(INM,4),ND(1)
FORMAT(1X,I15,8F10.2)
FORMAT(1HO)
DO 50 I=1,N
CJ(I)=(,0,0)
K=JA(I)
DO 40 KK=1,2
KA=IA(K)
KB=IB(K)
JJ=K
F1=1.
IF (KB.EQ,I2(I))GO TO 36
IF (KB.EQ,I1(I))F1=-1.
CJ(I)=CJ(I)+F1*WG(JJ)
GO TO 40
IF (KA.EQ,I3(I))F1=-1.
JJ=K+NM
CJ(I)=CJ(I)+F1*WG(JJ)
K=JB(I)
CONTINUE
DO 55 I=1,N
CG(I)=CJ(I)
CALL SQROT(C,CJ,0,I12,N)
I12=2
YI1=(,0,0)
DO 80 I=1,N
YI1=YI1+CJ(I)*CONJG(CG(I))
CALL RITE(IA,IB,INM,IMR,I1,I2,I3,MD,ND,NM,CJ,CG)
ZI1=1./YI1
PIN=GG
GDISS(AM,CG,CMH,DD,DISS,GAM,NM,SGD,ZLD,ZS)
PRAD=PIN-DISS
EFF=100.*PRAD/PIN
RETURN
END

```

Fig. 15. Subroutine GANTI

```

SUBROUTINE SQROT(C,S,IMR,I12,NEQ)
0001
0002
0003
0004
0005
0006
0007
0008
0009
0010
0011
0012
0013
0014
0015
0016
0017
0018
0019
0020
0021
0022
0023
0024
0025
0026
0027
0028
0029
0030
0031
0032
0033
0034
0035
0036
0037
0038
0039
0040
COMPLEX C(I),S(I),SS
FORMAT(1X,I15,1F10.3,1F15.7,1F10.0,2F15.0)
FORMAT(1HO)
N=NEQ
IF (I12.EQ,2)GO TO 20
C(I)=CSORT(C(I))
DO 4 K=2,N
C(K)=C(K)/C(1)
DO 10 I=2,N
IMO=I-1
IP0=I+1
ID=(I-1)*N-(I*1-1)/2
I1=ID+1
DO 5 L=1,IMO
LI=(L-1)*N-(L*L-L)/2+1
C(I1)=C(I1)-C(LI)*C(LI)
C(I1)=CSORT(C(I1))
IF (IP0.GT,N)GO TO 10
DO 8 J=IP0,N
IJ=ID+J
DO 6 M=1,IMO
MD=(M-1)*N-(M*M-M)/2
MI=MD+1
MJ=MD+J
C(I1)=C(I1)-C(MJ)*C(MJ)
C(IJ)=C(IJ)/C(I1)
CONTINUE
DO 30 I=2,N
IMO=I-1
DO 25 L=1,IMO
LI=(L-1)*N-(L*L-L)/2+1
S(I1)=S(I1)-C(LI)*S(L)
I1=(I-1)*N-(I*1-1)/2+1
S(I1)=S(I1)/C(I1)
NM=(N+1)*N/2
S(N)=S(N)/C(NN)
NMO=N-1
DO 40 I=1,NMO
KD=K-1
K=N-1
KPO=K+1
DO 35 L=KPO,N
KL=KD+L
SK(K)=S(K)-C(KL)*S(L)
KK=KD+K
SK(K)=S(K)/C(KK)
IF (IMR.LE,0) GO TO 100
CNOR=0
DO 50 I=1,N
SA=CABS(S(I))
IF (SA.GT,CNOR)CNOR=SA
IF (CNOR.LE,0.)CNOR=1.
DO 60 I=1,N
SS=S(I)
SA=CABS(SS)
SNOR=SA/CNOR
PH=0
IF (SA.GT,0.)PH=57.29578*ATAN2(AIMAG(SS),REAL(SS))
WRITE(6,2)I,SNOR,SA,PH,SS
WRITE(6,3)
100 RETURN
END

```

Fig. 16. Subroutine SQROT

matrix. On entry to SQROT, the upper-right triangular portion of  $Z(I,J)$  is stored by rows in  $C(K)$  with

$$(4) \quad K = (I - 1) * NEQ - (I * I - 1) / 2 + J$$

If  $I12 = 1$ , SQROT will transform the symmetric matrix into the auxiliary matrix (implicit inverse), store the result in  $C(K)$  and use the auxiliary matrix to solve the simultaneous equations. If  $I12 = 2$ , this indicates that  $C(K)$  already contains the auxiliary matrix.

The transformation from the symmetric matrix to the auxiliary matrix is programmed above statement 10, and the solution of the simultaneous equations is programmed in statements 20 to 40. If IWR is positive, the program below statement 40 will write the solution.

SQROT uses the square root method described in Reference 4. The original symmetric matrix  $Z$  and the upper triangular auxiliary matrix  $A$  are related by

$$(5) \quad Z = A' A$$

where  $A'$  is the transpose of  $A$ .

In the thin-wire application, SQROT must be called with  $I12 = 1$  before it is called with  $I12 = 2$ . With a large matrix, the execution time in SQROT is much smaller with  $I12 = 2$  than with  $I12 = 1$ .

#### APPENDIX 10. Subroutine RTE

Subroutine RTE is listed in Fig. 17. Given the list of loop currents  $CJ(I)$ , this subroutine generates a list of branch currents  $CG(J)$ .  $CG(J)$  and  $CG(JJ)$  denote the currents at  $IA(J)$  and  $IB(J)$ , respectively, on the wire segment  $J$ , where  $JJ = J + NM$ . If IWR is a positive integer, the program below statement 110 writes a list of the branch currents. The symbols in this list are defined as follows:

K	the segment number
ACJ	normalized current magnitude at $IA(K)$
BCJ	normalized current magnitude at $IB(K)$
PA	phase of current at $IA(K)$
PB	phase of current at $IB(K)$
CJA	complex current at $IA(K)$
CJB	complex current at $IB(K)$

The phase angles PA and PB are in degrees. Even if IWR is negative, RTE generates the branch-current list for use in subroutine GDISS.

```

SUBROUTINE RTE(IA,IB,INM,IWR,I1,I2,I3,I4,MD,NM,NK,CJ,CG)
  COMPLEX CJ(1),CG(1),CJA,CJB
  DIMENSION IA(1),IB(1),I1(1),I2(1),I3(1),MD(1NM,4),ND(1)
  FORMAT(1X,15,2F10.3,2F10.0,4F15.6)
  FORMAT(1H0)
  AMAX=.0
  DO 100 K=1,NM
    KA=IA(K)
    KB=IB(K)
    CJA=(.0,.0)
    CJB=(.0,.0)
    NDK=ND(K)
    DO 40 I1=1,NDK
      I=MD(K,I1)
      F1=1.
      IF (KB.EQ.I2(I)) GO TO 36
      IF (KB.EQ.I1(I)) F1=-1.
      CJA=CJA+F1*CJ(I)
      GO TO 40
      IF (KA.EQ.I3(I)) F1=-1.
      CJB=CJB+F1*CJ(I)
    CONTINUE
    CG(K)=CJA
    KK=K+NM
    CG(KK)=CJB
    ACJ=CABS(CJA)
    BCJ=CABS(CJB)
    IF (ACJ.GT.AMAX) AMAX=ACJ
    IF (BCJ.GT.AMAX) AMAX=BCJ
  CONTINUE
  IF (IWR.GT.0) GO TO 110
  RETURN
110 IF (AMAX.LE.0.) AMAX=1.
  DO 200 K=1,NM
    CJA=CG(K)
    KK=K+NM
    CJB=CG(KK)
    ACJ=CABS(CJA)/AMAX
    BCJ=CABS(CJB)/AMAX
    PA=57.29578*ATAN2(AIMAG(CJA),REAL(CJA))
    PB=57.29578*ATAN2(AIMAG(CJB),REAL(CJB))
  WRITE(6,2) K,ACJ,BCJ,PA,PB,CJA,CJB
  RETURN
END

```

Fig. 17. Subroutine RTE

## APPENDIX 11. Subroutine GDISS

Subroutine GDISS is listed in Fig. 18. This subroutine uses Eq. 50 of Reference 1 to calculate the time-average power dissipated in the imperfectly conducting wire. This is accomplished in the DO LOOP terminating at statement 100. The power dissipated in the lumped loads is calculated in the DO LOOP terminating with statement 140. DISS denotes the time-average power dissipated in the wire and the loads.

## APPENDIX 12. Subroutine GNFLD

Subroutine GNFLD, listed in Fig. 19, inputs the loop currents  $CJ(1)$ , calls GNF for the near-zone field of each wire segment, and sums over all the segments to obtain the near-zone field of the wire antenna or the near-zone scattered field of the wire scatterer.  $EX$ ,  $EY$  and  $EZ$  denote the cartesian components of this field at the observation point  $(X, Y, Z)$ . This calculated field does not include the incident fields of the magnetic frills or loops associated with generators on the antenna. It also does not include the radiation from the polarization currents in the dielectric insulation.

This subroutine could be simplified and speeded by inputting the branch currents  $CG(I)$  instead of the loop currents  $CJ(1)$ . However, this would increase the storage requirements because the far-field subroutine GNFLD would have to store the branch currents induced by the phi-polarized and theta-polarized incident waves.

## APPENDIX 13. Subroutine GNF

Subroutine GNF, listed in Fig. 20, uses Eqs. 75 and 76 of Reference 1 to calculate the near-zone electric field of a sinusoidal electric monopole with endpoints at  $(XA, YA, ZA)$  and  $(XB, YB, ZB)$ . The observation point is at  $(X, Y, Z)$ .  $EX1$ ,  $EY1$  and  $EZ1$  are the components of the field generated by the mode with unit current at  $(XA, YA, ZA)$ .  $EX2$ ,  $EY2$  and  $EZ2$  denote the field generated by the mode with unit current at  $(XB, YB, ZB)$ . GNF is similar to GGS, and Appendix 5 defines many of the symbols used in both subroutines.

## APPENDIX 14. Subroutine GFELD

The far-field subroutine GFELD, listed in Fig. 21, is discussed in section II. In antenna gain calculations with  $INC = 0$ , the loop currents  $CJ(1)$  are employed by GFELD to calculate the far-zone field. The field of each segment is obtained by calling GNF, and a summation over all the segments yields the field of the antenna.

In a bistatic scattering situation with  $INC = 2$ , the input data include the loop currents  $EP$  and  $ET$  induced by phi-polarized and theta-polarized incident waves. These currents were calculated by GFELD in a

```

SUBROUTINE GDISS(AM,CG,CMH,D,DISS,GM,NM,SGD,ZLD,ZS)
  COMPLEX CG(1),SGD(1),ZLD(1),CJA,CJB,GM,ZS
  DIMENSION D(1)
  DATA P1/3.14159/
  DISS=0
  IF (CMH.LE.0.)GO TO 120
  ALPH=REAL(GAM)
  BETA=AIMAG(GAM)
  RH=REAL(ZS)/(4.*PI*AM)
  DO 100 K=1,NM
    DK=D(K)
    DEN=CABS(SGD(K))**2
    EAD=EXP(1ALPH*DK)
    CAD=(EAD+1./EAD)/2.
    CSD=COS(BETA*DK)
    SAD=DK
    IF (ALPH.NE.0.)SAD=(EAD-1./EAD)/(2.*ALPH)
    SBD=DK
    IF (BETA.NE.0.)SBD=SIN(BETA*DK)/BETA
    FA=RH*(SAD*CAD-SBD*CBD)/DEN
    FB=2.*RH*(CAD*SBD-SAD*CBD)/DEN
    CJA=CG(K)
    L=K+NM
    CJB=CG(L)
    100 DISS=DISS+FA*(CABS(CJA)**2+CABS(CJB)**2)
    2+FB*(REAL(CJA)*REAL(CJB)+AIMAG(CJA)*AIMAG(CJB))
  120 DO 140 J=1,NM
    K=J+NM
    140 DISS=DISS+REAL(ZLD(J))*(CABS(CG(K))**2)
    2+REAL(ZLD(K))*(CABS(CG(K))**2)
  RETURN
END

```

Fig. 18. Subroutine GDISS

```

SUBROUTINE GNF LD(IA,IB,INM,11,12,13,MD,N,ND,NM,AM,CGD,SGD,ETA,GAM
2,CJ,D,X,Y,Z,XP,YP,ZP,EX,EY,EZ)
COMPLEX EX,EY,EZ,EX1,EY1,EZ1,EX2,EY2,EZ2,ETA,GAM
COMPLEX CJ(1),CGD(1),SGD(1)
DIMENSION IA(1),IB(1),11(1),12(1),13(1),D(1),X(1),Y(1),Z(1)
DIMENSION MD(INM+4),ND(1)
DATA P1,P/3,14159,6,28318/
EX=(.0,.0)
EY=(.0,.0)
EZ=(.0,.0)
DO 140 K=1,NM
KA=IA(K)
KB=IB(K)
CALL GNF(X(KA),Y(KA),Z(KA),X(KB),Y(KB),Z(KB),XP,YP,ZP,AM,D(K)
2,CGD(K),SGD(K),ETA,GAM,EX1,EY1,EZ1,EX2,EY2,EZ2)
NDK=ND(K)
DO 140 I=1,NDK
I=MD(K,11)
FI=1.
IF(KB.EQ.12(1))GO TO 136
IF(KB.EQ.11(1))FI=-1.
EX=X+FI*EX1*CJ(1)
EY=Y+FI*EY1*CJ(1)
EZ=EZ+FI*EZ1*CJ(1)
GO TO 140
136 IF(KA.EQ.13(1))FI=-1.
EX=X+FI*EX2*CJ(1)
EY=Y+FI*EY2*CJ(1)
EZ=EZ+FI*EZ2*CJ(1)
140 CONTINUE
RETURN
END

```

Fig. 19. Subroutine GNF LD

```

0001
0002
0003
0004
0005
0006
0007
0008
0009
0010
0011
0012
0013
0014
0015
0016
0017
0018
0019
0020
0021
0022
0023
0024
0025
0026
0027
0028
0029
0030
0031
0032

```

```

SUBROUTINE GNF(XA,YA,ZA,XB,YB,ZB,X,Y,Z,AM,DS,CGDS,SGDS,ETA,GAM
2,EX1,EY1,EZ1,EX2,EY2,EZ2)
COMPLEX EJA,EJB,EJ1,EJ2,ER1,ER2,ES1,ES2,SGDS,GAM,CT,CGDS,ETA
COMPLEX EX1,EY1,EZ1,EX2,EY2,EZ2
DATA P1/P/3,14159/
CAS=(XB-XA)/DS
CBS=(YB-YA)/DS
CGS=(ZB-ZA)/DS
SZ=(X-XA)*CAS+(Y-YA)*CBS+(Z-ZA)*CGS
ZL1=SZ
ZL2=SZ-DS
XXZ=X-XA-SZ*CAS
YYZ=Y-YA-SZ*CBS
ZZZ=Z-ZA-SZ*CGS
RS=XXZ**2+YYZ**2+ZZZ**2
R1=SQRT(RS+ZL1**2)
EJA=EXP(-GAM*R1)
EJ1=EJA/R1
R2=SQRT(RS+ZL2**2)
EJB=EXP(-GAM*R2)
EJ2=EJB/R2
ES1=EJ2-EJ1*CGDS
ES2=EJ1-EJ2*CGDS
ER1=(.0,.0)
ER2=(.0,.0)
AMS=AM*AM
IF(RS.LT.AMS)GO TO 80
CTH1=ZZ1/R1
CTH2=ZZ2/R2
ER1=(EJA*SGDS+EJA*CGDS*CTH1-EJB*CTH2)/RS
ER2=(EJB*SGDS+EJB*CGDS*CTH2-EJA*CTH1)/RS
CST=ETA/(4.*PI*SGDS)
EX1=CST*(ES1*CAS+ER1*XXZ)
EY1=CST*(ES1*CBS+ER1*YYZ)
EZ1=CST*(ES1*CGS+ER1*ZZZ)
EX2=CST*(ES2*CAS+ER2*XXZ)
EY2=CST*(ES2*CBS+ER2*YYZ)
EZ2=CST*(ES2*CGS+ER2*ZZZ)
RETURN
END

```

Fig. 20. Subroutine GNF



```

SUBROUTINE GFFLD(IA,IB,INC,INM,IMR,II,IZ,I3,I12,I3,I12,MD,N,ND,NM,AM
2,ACSP,ACST,C,CGO,CG,CJ,CMM,D,ECSP,ECST,EP,ET,EP2,ET2,EPPS,EPTS
3,ETPS,ETTS,GG,GPP,GTT,PH,SGO,SCSP,SCST,SPPM,SPTH,STPM,STTH,TH
4,X,Y,Z,ZLD,ZS,ETA,GAM)
COMPLEX CJ1,ET1,ET2,EP1,EP2,EPPS,ETTS,EPTS,ETPS,ZS,VP,VT
COMPLEX CJ1,CJ11,EP11,ET11,ET11,EP11,ET11,ET11,ZLD(1)
COMPLEX ETA,GAM,CGO(1),SGO(1),CG(1)
DIMENSION IAL(1),IB(1),II(1),I2(1),I3(1),I3(1),MD(INM,4)
DATA P1,P1/3,14,159,6,28318/
CJ1=-4.*PI/ETA*GAM)
GGG=REAL(1./ETA)
THR=.0174533*TH
CTH=COS(THR)
STH=SIN(THR)
PHR=.0174533*PH
CPH=COS(PHR)
SPH=SIN(PHR)
DO 130 I=1,N
ET1(1)=(0.,0)
DO 140 K=1,NM
KA=IA(K)
KB=IB(K)
CALL GFEX(KA),Y(KA),Z(KA),X(KB),Y(KB),Z(KB),D(K)
2,CGO(K),SGO(K),CTH,STH,CPH,SPH,6*AM,ETA,ET1,ET2,EP1,EP2)
NDK=ND(K)
DO 140 II=1,NDK
I=MD(K,II)
F1=1.
IF (KB.EQ.12(1))GO TO 136
IF (KB.EQ.11(1))F1=-1.
EPP11=EPP(1)+F1*EP1
ET11=ET(1)+F1*ET1
GO TO 140
136 IF (KA.EQ.13(1))F1=-1.
EPP11=EPP(1)+F1*EP2
ET11=ET(1)+F1*ET2
140 CONTINUE
EPPS=(0.,0)
ETTS=(0.,0)
IF (INC.EQ.0)GO TO 200
IF (INC.EQ.2)GO TO 170
DO 150 I=1,N
ET11=ET(1)*CJ1
EPT11=EPP(1)*CJ1
150 CALL SOROTC,EP,0,112,N)
112=2
CALL SOROTC,ET,0,112,N)
CALL RITE(IA,IB,INM,IMR,II,IZ,I3,MD,ND,NM,EP,CG)
CALL GDISS(AM,CG,CMM,D,PDIS,GAM,NM,SGO,ZLD,ZS)
CALL RITE(IA,IB,INM,IMR,II,IZ,I3,MD,ND,NM,ET,CG)
CALL GDISS(AM,CG,CMM,D,TDIS,GAM,NM,SGD,ZLD,ZS)
ACSP=PDIS/666
ACST=TDIS/666
PIN=.0
TIN=.0
DO 164 I=1,N
VP=CJ1*EPP(1)
VT=CJ1*ET(1)
PIN=PIN+REAL(VP*CONJG(ET11))
164 TIN=TIN+REAL(VT*CONJG(ET11))

```

Fig. 21a. Subroutine GFFLD

46

```

0001
0002
0003
0004
0005
0006
0007
0008
0009
0010
0011
0012
0013
0014
0015
0016
0017
0018
0019
0020
0021
0022
0023
0024
0025
0026
0027
0028
0029
0030
0031
0032
0033
0034
0035
0036
0037
0038
0039
0040
0041
0042
0043
0044
0045
0046
0047
0048
0049
0050
0051
0052
0053
0054
0055
0056
0057
0058
0059
0060
0061
0062

ECS=PIN/666
ECST=TIN/666
SCSP=ECSP-ACSP
SCST=ECST-ACST
EPTS=(0.,0)
ETPS=(0.,0)
DO 180 I=1,N
EPPS=EPPS+EP(1)*EPP(1)
EPTS=EPTS+EP(1)*ET(1)
ETTS=ETTS+ET(1)*ET(1)
ETPS=ETPS+ET(1)*EPP(1)
SPPM=2.*TP*(CABS(EPPS)**2)
STPM=2.*TP*(CABS(ETPS)**2)
STPM=2.*TP*(CABS(ETPS)**2)
STPM=2.*TP*(CABS(ETPS)**2)
RETURN
DO 260 I=1,N
ETTS=ETTS+CJ11*ET(1)
EPPS=EPPS+CJ11*EPP(1)
APP=CABS(EPPS)
ATT=CABS(ETTS)
GPP=4.*PI*APP*APP*GGG/66
GIT=4.*PI*ATT*ATT*GGG/66
RETURN
END

```

Fig. 21b. Subroutine GFFLD

47

previous call for the backscattering situation with INC = 1. Thus, a bistatic call must be preceded by a backscatter call.

EPP(1) and ETT(1) denote the phi-polarized and theta-polarized far-zone fields of dipole mode 1 with unit terminal current. In a backscattering situation, the excitation voltages EP(1) and ET(1) are obtained by multiplying EPP and ETT by the constant CJI. (See Eqs. 38, 39 and 40 in Reference 1.) Then calls are made to SQR0T which stores the solution (the induced loop currents) in EP(1) and ET(1). RTE is called for the branch currents CG(J), and GDISS is called for the time-average power dissipated in the imperfectly conducting wire and the lumped loads. This power is denoted PDIS and TDIS for phi-polarized and theta-polarized incident waves, respectively.

In scattering problems, the incident plane wave has unit electric field intensity at the coordinate origin. GGG denotes the time-average power density of the incident wave at the origin. ACSF and ACST denote the absorption cross sections for the phi and theta polarizations.

PIN and TIN denote the time-average power input to the wire structure, delivered by the equivalent voltage generators VP and VT at the terminals. PIN and TIN apply for the phi and theta polarizations, respectively. The time-average power input is regarded as the sum of the time-average power dissipated (in the wire and the lumped loads) and the time-average power radiated or scattered by the wire. ECSF and ECST denote the extinction cross sections and SCSF and SCST are the scattering cross sections.

The distant field is calculated in the D0 LOOP ending with statement 180 for scattering situations, and in the D0 LOOP ending with statement 260 for the antenna situation. In these fields, the range dependence is suppressed as in Eq. (1).

The radar cross sections (echo areas) SPPM, SPTM, STPM and STTM are defined as in Eq. 72 of Reference 1 with the incident power density (S<sub>i</sub> or GGG) evaluated at the coordinate origin. The user selects the location of the origin when supplying the input data for the coordinates of all the points on the wire.

For an antenna, the following definition is employed for the power gain:

$$(6) \quad G_0(\theta, \phi) = \lim_{r \rightarrow \infty} \frac{4\pi r^2 e^2 \alpha^2 S(r, \theta, \phi)}{P_i}$$

where P<sub>i</sub> (or GG in the program) denotes the time-average power input and S(r, θ, φ) is the time-average power density in the radiated field. For an antenna in a lossless medium, α vanishes and Eq. (6) reduces to the standard definition of power gain. Without the factor e<sup>2</sup>α<sup>2</sup> in Eq. (6), the power gain would vanish for a finite antenna in a conducting medium. GPP and GTT denote the power gains associated with the phi-polarized and theta-polarized components of the field, respectively.

## APPENDIX 15. Subroutine GFF

Subroutine GFF, listed in Fig. 22, uses the equations in Appendix 2 of Reference 1 to calculate the far-zone field of a sinusoidal electric monopole. The monopole has endpoints (XA, YA, ZA) and (XB, YB, ZB). EP1 and ET1 denote E<sub>φ</sub> and E<sub>θ</sub> for the mode with unit current at (XA, YA, ZA). EP2 and ET2 denote the fields for the mode with unit current at (XB, YB, ZB). The range dependence is suppressed as in Eq. (1). The far field vanishes in the endfire direction where GK = 0.

```

SUBROUTINE GFF (XA,YA,ZA,XB,YB,ZB,D,
2CGD,SGD,CTH,STH,CPH,SPH,
ZGAM,ETA,ET1,ET2,EPI,EP2)
COMPLEX ET1,ET2,EPI,EP2,GAM,ETA
COMPLEX GD,CGD,SGD,EGD
COMPLEX EGFA,EGFB,EGGD,ESB,ESB
COMPLEX CST
FP=12.56637
XAB=XB-XA
YAB=YB-YA
ZAB=ZB-ZA
CA=XAB/D
CB=YAB/D
CG=ZAB/D
G=(CA*CPH+CB*SPH)*STH+CG*CTH
GK=1.-G*G
ET1=(.0,.0)
ET2=(.0,.0)
EPI=(.0,.0)
EP2=(.0,.0)
IF (GK.LT..001)GO TO 200
FA=(XA*CPH+YA*SPH)*STH+Z*CTH
FB=(XB*CPH+YB*SPH)*STH+ZB*CTH
EGFA=CEXP(GAM*FA)
EGFB=CEXP(GAM*FB)
EGGD=CEXP(GAM*GD)
CST=ETA/(GK*SGD*P)
ESB=CST*EGFA*(EGGD-G*SGD-CGD)
ESB=CST*EGFB*(1./EGGD+G*SGD-CGD)
T=(CA*CPH+CB*SPH)*CTH-CG*STH
P=-CA*SPH+CB*CPH
ET1=T*ESA
ET2=T*ESB
EPI=P*ESA
EP2=P*ESB
200 CONTINUE
RETURN
END

```

Fig. 22. Subroutine GFF